

# Describing Trotterized Time Evolutions on Noisy Quantum Computers via Static Effective Lindbladians

Keith R. Fratus, Kirsten Bark, Nicolas Vogt, Juha Leppäkangas, Sebastian Zanker, Michael Marthaler, and Jan-Michael Reiner

HQS Quantum Simulations GmbH, Haid-und-Neu-Straße 7, 76131 Karlsruhe, Germany

**We consider the extent to which a noisy quantum computer is able to simulate the time evolution of a quantum spin system in a faithful manner. Given a common set of assumptions regarding the manner in which noise acts on such a device, we show how the effects of noise can be reinterpreted as a modification to the dynamics of the original system being simulated. In particular, we find that this modification corresponds to the introduction of static Lindblad noise terms, which act in addition to the original unitary dynamics. The form of these noise terms depends not only on the underlying noise processes occurring on the device, but also on the original unitary dynamics, as well as the manner in which these dynamics are simulated on the device, i.e., the choice of quantum algorithm. We call this effectively simulated open quantum system the noisy algorithm model. Our results are confirmed through numerical analysis.**

## 1 Introduction

Simulating the time evolution of quantum systems is widely discussed as one of the prime applications of quantum computers due to the exponential speedup these new devices promise over conventional computers [1–3]. However, so far the error rates on present universal devices prohibit solving more than small-scale example systems [4–7]. Furthermore, quantum error correction is out of reach for the near future [8–10]. Hence, research regarding early utilization of quantum computers often focuses on algorithms with low circuit depth [11], and on mitigating errors rather than trying to remove them [12, 13]. In this endeavor of enabling near-future useful quantum computing, it is crucial to understand the effects that noise can have on the results of a simulation performed on such a device. We have investigated this question already in earlier work for specific noise types and quantum systems [14]. Here, we present a more extensive approach to this problem.

We focus in this work on the time evolution of quantum spin systems – systems described by a Hamiltonian in which a number of spin degrees of free-

dom experience few-body interactions among each other. A wide variety of physical systems are well-approximated by such a description, but solving quantum spin systems is in general hard, either analytically or using conventional computers [15, 16]. Since there exists a direct mapping between spin degrees of freedom and qubits on a quantum device, such a time-evolution can be implemented in a natural fashion on such a device using the Suzuki-Trotter decomposition and the natively available gate set [2, 17]. However, the presence of noise will result in gate operations which are not faithful representations of their intended unitary operations, and thus in turn will alter the true time evolution of the quantum register.

Our aim in the present work is to understand how the effects of noise on such a time evolution can be interpreted as a modification to the dynamics driving this time evolution. We demonstrate that, given a common set of assumptions regarding the noise processes acting on the device, these modifications can be well-approximated by the introduction of static Lindblad noise terms, which act in addition to the existing unitary dynamics. The nature of these Lindblad terms depends on the noise present on the device, but also on the particular choice of Hamiltonian dynamics, as well as the manner in which these Hamiltonian dynamics are implemented on the device as a sequence of gate operations, i.e., the quantum algorithm. For this reason, we call the resulting effective Lindbladian the *noisy algorithm model*.

The outline of this paper is as follows: In Section 2 we discuss the types of spin systems and quantum algorithms considered in our analysis, and in Section 3 we outline our assumptions regarding the nature of the noise on the devices we consider. The main results of our analysis are how to derive the noisy algorithm model and what its properties are. We present these results in Section 4, while a numerical analysis of them is given in Section 5. We conclude in Section 6. After the main text, we give more detailed information about the rationale behind our noise assumptions in Appendix A, followed in Appendix B by derivations of the formulas we use to calculate the Lindblad terms of the noisy algorithm model. Furthermore, in Appendix C we describe our software implementation of the presented method, and finally give an extensive discussion of the errors of our model in Appendix D.

arXiv:2210.11371v1 [quant-ph] 20 Oct 2022

## 2 Time Evolution of Spin Systems

We will restrict ourselves to circuits which involve the digital quantum simulation of the time evolution of a quantum system comprised of a set of spin- $\frac{1}{2}$  degrees of freedom, with the Hamiltonian

$$H = \sum_X h_X. \quad (1)$$

Each subset  $X$  is limited to a non-extensive number of spins (in practice two spins at most), and  $h_X$  describes the interactions among these spins. For a system with  $n$  spins, the Hilbert space  $\mathcal{H}$  has dimension  $\mathcal{D} = 2^n$ . For simplicity, we will assume that the Hamiltonian is time-independent, although the generalization of our results to the time-dependent case is straightforward. A common example of such a Hamiltonian would be the Transverse-Field Ising Model with nearest-neighbor interactions,

$$H = J \sum_{\langle ij \rangle} \sigma_i^z \sigma_j^z + g \sum_i \sigma_i^x, \quad (2)$$

the physics of which depends strongly on the geometry of the underlying lattice. Since the degrees of freedom in the Hamiltonian are spin- $\frac{1}{2}$  observables, it is possible to associate each degree of freedom with a qubit on a quantum device, without the need for additional transformations (for example, the Jordan-Wigner transformation in the case of fermionic degrees of freedom).

To perform such a digital simulation, the unitary time evolution is approximated using the usual Trotter expansion [18–20],

$$\begin{aligned} U(t) &= \exp(-iHt) = \prod_{n=1}^N \exp(-iH\tau) \\ &\approx \prod_{n=1}^N \prod_X \exp(-ih_X\tau) \equiv \prod_{n=1}^N \prod_X U_X(\tau) \end{aligned} \quad (3)$$

where  $\tau = t/N$ . Such a Trotter expansion of course involves some degree of approximation. The true Hamiltonian being simulated in such a time evolution can be found using the *Baker-Campbell-Hausdorff* (BCH) formula, which to first order in the Trotter step size is given according to

$$H \rightarrow H_{\text{eff}} = H + \delta H = \sum_X h_X - \frac{i}{2}\tau \sum_{X<Y} [h_X, h_Y], \quad (4)$$

where  $X < Y$  when the term  $h_X$  appears to the left of  $h_Y$  in the Trotter product. Since the individual terms  $h_X$  in the Hamiltonian involve only a small number of sites, the unitary operators appearing as products in the Trotterized time evolution can be efficiently simulated using gates natively available on a quantum device [2, 17].

## 3 Assumptions Regarding Noise in a Quantum Circuit

Throughout the implementation of a Trotter step, decoherence will lead to the accumulation of errors in our simulation. In order to analyze the effects of this noise, we must assume a model for how noise manifests itself at the circuit level. Our assumption throughout this work will be that the effects of noise can be accounted for at the level of individual gates. In particular, we will assume that a circuit can be modeled as a sequence of noise-free quantum gates,  $\{G\}$ , with each gate followed by an individual, discrete decoherence event  $\mathcal{N}_G$ , which leads to some decoherence of the device register.

The form of the discrete noise following a gate will of course depend on the particular choice of gate, and the particular choice of hardware. We will assume that the form of this noise is known (perhaps as a result of tomography performed on the relevant device), and remains constant throughout at least a single run. We will also assume that the noise event which occurs after a gate affects only those qubits which are involved in the gate - in other words, the noise following a gate operation on a set of qubits does not lead to any entanglement with any of the other qubits on the device. Note that this framework includes the noise accumulated on qubits as they idle, when accounting for the action of the “trivial” gate (in other words, the action of doing nothing to a qubit).

To account for the effects of noise in our simulation in concrete terms, we must adopt the notation of the density matrix, rather than the pure wave function, which cannot describe the evolution of mixed quantum states. In the strictly unitary case in which the density matrix remains pure, this replacement can be made according to

$$\begin{aligned} |\psi(t)\rangle &\rightarrow \rho(t) = |\psi(t)\rangle\langle\psi(t)| \Rightarrow \\ \exp(-iHt) |\psi(0)\rangle &\rightarrow \exp(-iHt) \rho(0) \exp(+iHt) \end{aligned} \quad (5)$$

Using the identity,

$$e^{\text{ad}_X} Y = e^X Y e^{-X}; \quad \text{ad}_X \equiv [X, \cdot], \quad (6)$$

the expression for the time-evolution of the density matrix can be further rewritten as,

$$\rho(t) = e^{\mathcal{L}_H t} \rho_0, \quad (7)$$

where the Liouvillian super-operator for the time-evolution of the density matrix is a linear operator acting on the space of density matrices, given as

$$\mathcal{L}_H \equiv -i \text{ad}_H = -i [H, \cdot] \quad (8)$$

Moving beyond the unitary case, the density matrix will, in general, no longer remain pure,

$$\text{Tr} [\rho^2(t)] \neq 1. \quad (9)$$

However, in order to respect the basic statistical interpretation of quantum mechanics, the density matrix must remain a positive semi-definite matrix with unit trace. In other words, the time-evolution of the density matrix must be a *completely positive, trace-preserving* (CPTP) map. The most general linear CPTP map on the space of density matrices, which also satisfies the property of generating Markovian time evolution, is given by the so-called Lindblad equation [21],

$$\mathcal{L}\{\rho\} = \mathcal{L}_H\{\rho\} + \mathcal{L}_D\{\rho\} = -i[H, \rho] + \sum_{n,m} \Gamma_{nm} \left( A_n \rho A_m^\dagger - \frac{1}{2} \{A_m^\dagger A_n, \rho\} \right) \quad (10)$$

The first term in this equation is recognizable as the original unitary evolution, while the second piece accounts for decoherence through noise. The operators  $\{A_n\}$  represent a basis for the space of all traceless operators on  $\mathcal{H}$ , while the *rate matrix*  $\Gamma$  must be Hermitian and positive semi-definite in order to preserve the statistical properties of the density matrix. The set of operators  $\{A_n\}$  is not unique - any basis of traceless operators is valid. Common choices include the generators of  $su(\mathcal{D})$  in the defining representation, or the set of all products of Pauli operators,

$$A_\alpha \equiv \bigotimes_{i=1}^n \sigma_i^{\alpha(i)} \quad (11)$$

Because the expression for the incoherent piece of the Lindblad equation is quadratic in the operators  $\{A_n\}$ , it can be diagonalized, leading to the more common diagonal form of the Lindblad equation,

$$\mathcal{L}_D\{\rho\} = \sum_i \gamma_i \left[ L_i(\rho) L_i^\dagger - \frac{1}{2} \{L_i^\dagger L_i, \rho\} \right], \quad (12)$$

where the  $\{\gamma_i\}$  are the eigenvalues of the rate matrix with eigenvectors  $\vec{v}_i$ , and

$$L_i = \sum v_i^{(n)} A_n. \quad (13)$$

Because the rate matrix is positive semi-definite, the eigenvalues  $\{\gamma_i\}$  will be non-negative. These eigenvalues represent the physical decay rates of the system under the effects of decoherence. More discussion of the Lindblad equation can be found in [22, 23].

Throughout this work, we will often refer to the overall “noise strength”, which for our purposes we define as

$$\gamma \equiv \text{Tr}[\Gamma]. \quad (14)$$

Note that this object is equal to the sum of the decay rates of the system.

With this in mind, we will assume that the decoherence event following the application of a gate can be modeled as Lindblad noise accumulating during a

small but finite time duration, namely the gate application time,

$$\mathcal{N}_G \rightarrow \exp(t_G \mathcal{L}_N^G), \quad (15)$$

where  $\mathcal{L}_N^G$  represents a term of pure Lindblad form (i.e., there is no Hamiltonian component). In appendix A, we argue for the validity of such a noise model for a wide variety of hardware implementations.

Having chosen a model for how the effects of noise manifest themselves at the level of a quantum circuit, we now proceed to analyze how this noise alters the effective model simulated by the circuit.

## 4 The Noisy Algorithm Model

Over the course of a single Trotter step, the state of the quantum register will have evolved from some initial  $\rho$ , to some final  $\rho'$ . In the ideal noise-free case, the evolution would correspond to the originally desired Hamiltonian time evolution,

$$\rho' = e^{\mathcal{L}_H \tau} \rho \quad (16)$$

However, the discrete noise terms occurring in the quantum circuit will result in a time-evolution which deviates from this ideal case. Our aim in this work is to describe these effects through an effective time-evolution operator

$$\rho' = e^{\mathcal{L}^{\text{eff}} \tau} \rho; \quad \mathcal{L}^{\text{eff}}\{\rho\} \equiv -i[H^{\text{eff}}, \rho] + \sum_{n,m} \Gamma_{nm}^{\text{eff}} \left( A_n \rho A_m^\dagger - \frac{1}{2} \{A_m^\dagger A_n, \rho\} \right), \quad (17)$$

and thereby interpret the quantum circuit as now performing a simulation of this effective model, the *noisy algorithm model*, rather than the original coherent model. We now proceed to characterize  $\mathcal{L}^{\text{eff}}$ , the principal component of the noisy algorithm model.

### 4.1 Circuits with Native Gates

To begin our analysis, we will assume that all of the exponential products in the Trotter expansion correspond to natively available gates on the given hardware. In other words, we will assume that the unitary operators

$$U_X(\tau) \equiv \exp(-i h_X \tau) \quad (18)$$

are natively available on the hardware as quantum logic gates (we will relax this assumption shortly). Written as a super-operator acting on the space of operators,

$$\mathcal{U}_X(\tau) \equiv e^{\mathcal{L}_X \tau}; \quad \mathcal{L}_X \equiv -i \text{ad}_{h_X} = -i[h_X, \cdot] \quad (19)$$

The Hamiltonian term  $h_X$  will generally consist of a term proportional to a product of Pauli operators, for example,

$$h_X = J_X \sigma_i^z \sigma_j^z, \quad (20)$$

where sites  $i$  and  $j$  live on the domain  $X$ . For the Trotter decomposition to be well-behaved, we must generally assume that the quantity

$$\phi_X = 2J_X\tau \quad (21)$$

is sufficiently small. Thus,  $U_X$  corresponds to the exponentiation of an argument which is parametrically small in the quantity  $\phi$ . We will refer to such an operation as a *small angle gate* (SAG).

All of these gate operations will of course have non-unitary dissipation terms interspersed among them. These terms also correspond to the exponentiation of an argument which is parametrically small in some quantity. In this case, however, the small quantity is the product of the gate time with the overall noise strength,

$$\mu_G = \gamma t_G. \quad (22)$$

For example, for independent dephasing noise on each qubit, the argument of this exponential term will be

$$\mathcal{L}_N^G \{\rho\} = \frac{\gamma t_G}{n} \sum_i (\sigma_i^z \rho \sigma_i^z - \rho). \quad (23)$$

In general, we will assume that

$$\mu_G \ll \phi_G \quad (24)$$

Without this assumption, the effects of noise on the device would be too great to perform any sort of useful computation.

Despite not being unitary, the noise terms are still generated through exponentiation of some linear (super) operator, and hence it is still possible to combine a noise term and a coherent gate term into a single exponential,

$$e^{t_G \mathcal{L}_N^G} e^{\tau \mathcal{L}_X} \rightarrow e^{\tau \mathcal{L}}, \quad (25)$$

where  $\tau \mathcal{L}$  is given according to the BCH formula. Since all of the noise and gate terms appearing in the circuit correspond to the exponentiation of “small” quantities, to lowest order in the BCH expansion we can combine all of these terms into a single exponential, by merely summing up all of their arguments,

$$\exp(\tau \mathcal{L}_{\text{eff}}) = \exp\left(\tau \sum_X \mathcal{L}_X + \sum_g t_g \mathcal{L}_N^g\right), \quad (26)$$

where the first summation is over all SAGs in the circuit, and the second summation is over all noise terms in the circuit (in this case where we only consider SAGs, these summations are in direct correspondence with each other). Dividing through by the Trotter step size  $\tau$ , we find

$$\mathcal{L}_{\text{eff}} \rightarrow \sum_X \mathcal{L}_X + \sum_g (t_g/\tau) \mathcal{L}_N^g. \quad (27)$$

The first term in this expression naturally corresponds to the originally desired time evolution (and so

to lowest order, there is no correction to the coherent dynamics). The second term represents the cumulative effects of all of the discrete noise terms occurring in the circuit. Thus, we find that we can interpret the effects of decoherence on the device as introducing an additional dissipative term to our simulated model,

$$\mathcal{L}_H = -i[H, \cdot] \rightarrow \mathcal{L}_{\text{eff}} = -i[H, \cdot] + \mathcal{L}_N \quad (28)$$

where

$$\mathcal{L}_N = \sum_g (t_g/\tau) \mathcal{L}_N^g. \quad (29)$$

The most prominent feature of this result is that the contribution to the effective noise from each discrete noise term depends on the ratio of gate time to simulated trotter step size. This is of course a familiar fact in the context of digital quantum simulation. From this perspective, larger gate times are problematic in the sense that they increase the effects of decoherence. From the perspective of utilizing noise as a resource, increased gate times are not necessarily problematic, as they simply adjust the model being simulated. However, it is in fact true that for long enough gate times, the effective noise may grow large enough that the time evolution can be effectively simulated on a classical computer, thus negating the need for a quantum approach and rendering the problem uninteresting.

## 4.2 Complications from “Large” Gates

So far, we have assumed that all gate operations occurring in our circuit correspond directly to a term appearing in the Trotter expansion,  $U_X(\tau)$ , parameterized by some small quantity. However, in reality, many of these terms  $U_X$  are not natively available as quantum gates on the hardware level, and must be decomposed into a set of available gates.

An example would be an Ising interaction term  $J\sigma_i^z\sigma_j^z$  from the Hamiltonian (2), where the exponential in the Trotter expansion can be implemented through a ZZ Ising gate via

$$e^{-iJ\sigma_i^z\sigma_j^z\tau} = e^{-i\frac{\phi}{2}\sigma_i^z\sigma_j^z} = \text{ZZ}(\phi), \quad (30)$$

with the angle  $\phi = 2J\tau$ . The ZZ gate can be decomposed using CNOTs and a rotation gate around the  $Z$  axis:

$$\text{ZZ}(\phi) = \text{CNOT}_{ij} \cdot \text{R}_{Z_j}(\phi) \cdot \text{CNOT}_{ij}, \quad (31)$$

where  $i$  is the control qubit, and  $j$  is the target qubit of  $\text{CNOT}_{ij}$  and the rotation is acting on the target qubit. Such a decomposition is illustrated in Figure 1. Another example is the use of Hadamard gates to modify a rotational axis,

$$\text{R}_Z(\phi) = \text{H} \cdot \text{R}_X(\phi) \cdot \text{H}, \quad (32)$$

illustrated in Figure 2. The key feature of these decompositions is that they involve gate operations

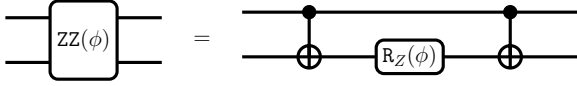


Figure 1: Demonstrating the idea of a block decomposition: A ZZ Ising gate can be decomposed into CNOT gates and a single qubit rotation around the  $Z$  axis.

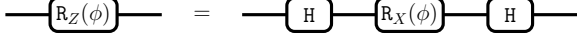


Figure 2: Another example of a gate decomposition: Using Hadamard gates to effectively change the axis of a rotation gate.

(here, for example, CNOT or Hadamard gates) which *cannot* be written as the exponentiation of some small term. We will therefore refer to such a sequence of gates as a *large gate decomposition block* (LGDB).

Since LGDBs contain terms which do not correspond to the exponentiation of some small parameter, simply summing together the exponential terms to first order in the BCH expansion is no longer a valid approximation. If we wish to analyze the effects of noise in circuits containing LGDBs using the techniques of the previous section, we must transform our circuit to one in which only small-angle Hamiltonian terms or noise terms exist. Such a transformation can be accomplished by identifying any noise terms occurring within a LGDB, and then shifting them to the outside of the block (while accounting for the effects of commuting these noise terms past any coherent gates within the block). Since the original LGDB, by definition, can be recombined back into a small angle term  $U_X(\tau)$ , we can then proceed with the original analysis. The goal, then, is to determine how the noise terms appearing within one of these LGDBs are modified by the process of commuting them to the outside of the block.

In concrete terms, we would like to solve the equation

$$e^{\mathcal{L}_G} e^{\mathcal{L}_N} = e^{\mathcal{L}_P} e^{\mathcal{L}_G}, \quad (33)$$

where  $\mathcal{L}_G$  describes the action of a noise-free gate,  $\mathcal{L}_N$  describes the original noise term, and  $\mathcal{L}_P$  describes the modified noise term we wish to find. This corresponds to moving a noise term in the circuit diagram from the left to the right of a gate, and is represented schematically in Figure 3. In Appendix B we derive a transformation which allows us to find the underlying rate matrix  $\Gamma^P$  of  $\mathcal{L}_P$  in terms of the rate matrix  $\Gamma^N$  of  $\mathcal{L}_N$ . This transformation is given according to

$$\Gamma^P = M\Gamma^N M^\dagger, \quad (34)$$

where we have defined the (unitary) matrix  $M$  as

$$M = \eta^{-1}\chi; \quad \chi_{mn} \equiv \text{Tr} \left[ A_m^\dagger U_G A_n U_G^\dagger \right]; \quad \eta_{mn} \equiv \text{Tr} \left[ A_m^\dagger A_n \right]. \quad (35)$$

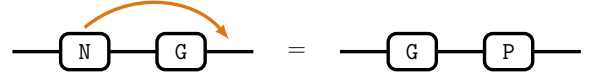


Figure 3: Demonstrating the idea of commuting noise past a gate  $G$ : The original noise term  $N$  that acted prior to  $G$  is replaced by a noise term  $P$  acting after  $G$ , where both gate sequences are equivalent. How to find  $P$ , given  $G$  and  $N$ , is explained in the main text.

Here the matrix  $U_G$  is the unitary matrix corresponding to the gate  $G$ , and the  $\{A_n\}$  are again the complete basis of traceless generators in the definition of the Lindblad equation. In the case that a noise term must be commuted past several gates, the transformation involves the matrix  $U$  which is the product of all of the corresponding unitary gate matrices,

$$U \equiv \prod_g U_g. \quad (36)$$

Since the matrix  $M$  is unitary, this transformation in fact preserves the noise spectrum.

We note that it is also possible to describe this noise transformation not through a change in the underlying rate matrix, but rather as a transformation of the basis  $\{A_n\}$ . Such a transformation takes the form

$$A_n \rightarrow E_n = U A_n U^\dagger. \quad (37)$$

This alternative picture may be useful in some computational contexts. For example, we use this formula in our software implementation to calculate the effective Lindblad terms, as mentioned in Appendix C.

With this information, we can now pass all noise terms to the outside of their corresponding LGDBs, and are left with a circuit containing only small angle gate terms and noise terms, allowing us to proceed with the original analysis, yielding

$$\mathcal{L}_H = -i[H, \cdot] \rightarrow \mathcal{L}_{\text{eff}} \equiv -i[H, \cdot] + \mathcal{L}_P \quad (38)$$

where now

$$\mathcal{L}_P \equiv \sum_g (t_g/\tau) \mathcal{L}_P^g. \quad (39)$$

A noise term  $\mathcal{L}_P^g$  appearing in the summation above may in fact correspond to one of the original  $\mathcal{L}_N^g$  when such a noise term need not be commuted past any large gates.

### 4.3 Handling SWAP Gates

So far, we have analyzed circuits with either small angle gate operations, or LGDBs which could be reduced to such small angle gate operations. Yet, there is a variety of circuits which cannot be reduced to such a paradigm. While a full treatment of all such cases is beyond the scope of this work, we focus here on a particularly prominent case - the use of SWAP gates to accommodate limited connectivity.

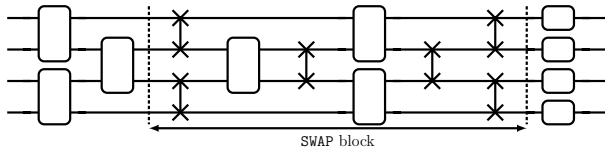


Figure 4: An example of a basic SWAP block, where between the swapping operations the qubit indices are effectively scrambled. This is to illustrate that treating SWAP blocks similarly to the decomposition blocks in Section 4.2 would easily lead to very large blocks, potentially causing a substantial computational overhead commuting all noise terms out of the block.

An example of such a circuit is shown in Figure 4. Here, we imagine that the four spins possess some pair interactions among themselves (the exact nature of this interaction is unimportant). If we assume only linear connectivity among the qubits on our chosen architecture, then the use of SWAP gates will be necessary to implement the pair interaction between spins which are not represented by adjacent qubits. This is indicated in the circuit diagram. We also imagine that some other gate operations occur which are designed to implement additional single-qubit Hamiltonian terms. Although not explicitly indicated on the diagram, the pair interaction terms may need to be decomposed into LGDBs. As usual, this case can be handled by commuting the noise terms within the block to the outside, as described previously. However, the SWAP gates themselves still pose a problem. If we follow the philosophy of the previous analysis, we must somehow manipulate our circuit so that only small angle gate operations and noise terms exist.

Of course, since the purpose of the SWAP gates is to account for pair interactions between non-adjacent spins, we know that, at least in the noise-free case, the circuit is equivalent to one in which the SWAPs are removed, and there exist pair interaction terms between the non-adjacent spins. It is clear then that this case can, at least in principle, be handled in a fashion similar to the previous case - one must simply commute out all of the noise terms which occur amid the various SWAP gates, so that the operations between the first and last SWAP gates can then be combined back into a sequence of operations which only contain small angle operations. In some sense, we can imagine the sequence of gates in between and including these SWAP gates as one combined decomposition block. In general, we will refer to such a sequence of gates as a *SWAP block*. In practice, however, computing one large transformation matrix  $M$  for all of the gate operations occurring within a SWAP block may become computationally demanding, especially for larger circuits. Even for the case of four spins, the dimensionality of the rate matrix implies that such transformations can generally be quite computationally demanding.

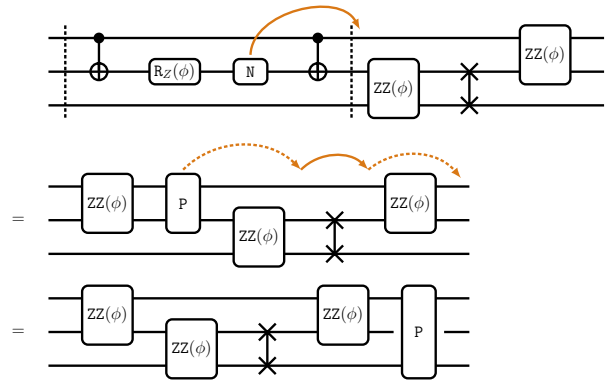


Figure 5: The two-step noise procedure for SWAP gates. First, noise terms appearing within a LGDB within the circuit need to be commuted out of the block. Here, this is indicated by the orange arrow in the first line: The noise  $N$  within the decomposition block between the dashed lines representing a ZZ Ising gate (see Figure 1) is shifted out of the block. After commuting  $N$  past the CNOT gate we are left with the (in general two-qubit) noise term  $P$  (similar to Figure 3). Now, the circuit consists only of LGDBs equivalent to small angle gates without noise, separate noise terms, and SWAPs. The second step is to commute  $P$  past all SWAPs. When doing this, moving past a LGDB (dashed orange arrows in the second line) does not modify  $P$ , moving past a SWAP gate (solid orange arrow in the second line) will change the qubits  $P$  is acting on.

Fortunately, handling SWAP blocks in such a way is not necessary – it is in fact possible to account for the effects of commuting a noise term outside of a SWAP block, without naively computing one giant transformation matrix; by splitting the block into LGDBs and SWAPs.

To see why, we first note that commuting a noise term past a small angle gate, to lowest (zero) order in the gate angle  $\phi$ , does not modify the noise (we will address this point in more detail shortly). Second, we note that the effect of commuting a noise term past a SWAP gate is to simply exchange the qubits participating in the noise term according to the SWAP operation. For this reason, the effects of commuting noise outside of (or past) a SWAP block can be accounted for in a two-step process. First, all noise terms occurring within an LGDB are commuted out of the LGDB, resulting in a circuit which now contains only noise, SWAP gates, and small angle gate operations. Second, all noise terms are commuted past the SWAP gates. In this second step, the only modifications to the noise terms we must account for are the qubit permutations which arise due to the SWAP gates, which does not require the computation of a transformation matrix  $M$ . Such a two-step process is indicated schematically in Figure 5.

Lastly, we comment on the need to account for swapping operations which occur without the use of explicit SWAP gates. Such a case is displayed in Fig-

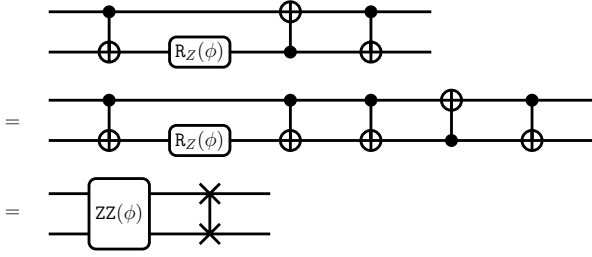


Figure 6: By adding an identity operation in the form of two CNOT gates into the gate sequence depicted at the top, one can find that this sequence is in fact equal to a ZZ Ising interaction as shown in Figure 1, followed by a SWAP gate (which can be decomposed into three alternating CNOTs).

ure 6. In the noise-free case, such a sequence of gates is equivalent to a pair-Z interaction, followed by a SWAP gate. Therefore, in order to treat this case, we must commute any noise terms to the outside of this gate sequence, replace the relevant gates with an effective small angle pair interaction followed by a SWAP gate, and then proceed with the previous analysis for handling SWAP blocks.

The issue of implicit swapping operations, as well as the fact that on quantum devices usually SWAP gates need to be decomposed into native hardware gates (e.g., three alternating CNOTs as in Figure 6), needs to be accounted for when analyzing circuits through software. Our software implementation circumvents these complications by adding an optional property to LGDBs that represent parametrically small gates within a Trotter step: A permutation, that accounts for implicit swapping within the LGDB. Commuting noise terms past a LGDB does not alter the noise type (which is valid within the Trotter approximation); it only alters the qubit indices the noise acts on, according to the given permutation.

In practice this captures all cases discussed in the above. More details on the software implementation of the paradigm laid out in this chapter are given in Appendix C.

#### 4.4 Scaling of Errors

We have thus far ignored the scaling of errors in our analysis. Here we briefly comment on this, while leaving a more detailed discussion to Appendix D.

There are two main sources of error to consider. The first source of error results from only summing to zero order in the BCH expansion. For the coherent dynamics, we find that this introduces an error of order  $J\tau$ , where  $\tau$  is again the Trotter step size, and  $J$  is some characteristic coupling scale of the Hamiltonian. For the noisy portion of the dynamics, we find an error of order  $\gamma t_G$ , where  $\gamma$  is the overall noise scale, and  $t_G$  is the characteristic gate time. If we

introduce, as in the above, the angle

$$\phi = 2J\tau, \quad (40)$$

then each of these corrections is of order  $\phi$  smaller than their dominant zero order contributions.

The second source of error results from naively commuting noise terms past small angle gates in SWAP blocks. We find that the error in this case is a contribution to the noisy dynamics, which is again a factor of  $\phi$  smaller than the dominant dynamics.

We note that when higher-order Suzuki-Trotter decompositions are utilized, additional care is required when considering the dominant sources of error. For the case of a second-order Suzuki-Trotter decomposition, we find that the errors introduced through our approximate noise model will be small compared with the errors introduced through Trotterization so long as

$$\gamma t_G \ll \phi^2. \quad (41)$$

## 5 Numerical Analysis

Having analyzed the effects of noise in our circuits, we now demonstrate the accuracy of our results. We will focus on the example circuit displayed in Figure 7, intended as a toy model for a circuit which could be analyzed with our methods. Such a circuit may correspond to the digital simulation of the time evolution of the transverse field Ising model,

$$H = J \sum_{\langle ij \rangle} \sigma_i^z \sigma_j^z + g \sum_i \sigma_i^x, \quad (42)$$

We assume that small angle Ising terms along the x-axis, as well as small angle single qubit rotations around the x-axis, are natively available on the device hardware. However, in contrast, we assume that only special large angles (for example, multiples of  $\pi/2$ ) are available for rotations along the y and z directions. Therefore, the use of Hadamard gates is necessary in order to implement interactions along more than one axis, which could be placed around either the Ising terms, or the single qubit terms. In this example, they are placed around the Ising terms, in order to accomplish an Ising interaction along the z axis.

We further assume a toy model for the implementation of a Hadamard gate, given according to

$$U_H = R_y(\pi/2)Z = \exp(-i\frac{\pi}{4}Y) \exp(-i\frac{\pi}{2}(I - Z)) \quad (43)$$

We also assume that the time required to implement a gate is roughly proportional to the gate angle. In particular, we will define  $t_R$  to be the time required to implement a  $\pi/2$  rotation. With this definition, the Hadamard gates have a gate time of  $t_g = 3t_R$ . Furthermore, we assume that at the underlying hardware

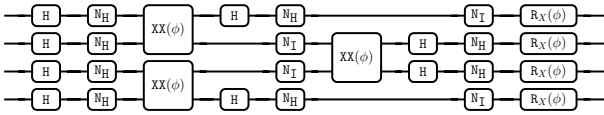


Figure 7: An example circuit that implements a Trotter step of the time evolution under the example Ising Hamiltonian 42. We defined  $\phi = 2J\tau = 2g\tau$ , with the parameters  $J$  and  $g$  from the Hamiltonian and the Trotter step size  $\tau$ . We assumed noise events happening when applying the large angle rotations for the Hadamard gate on a qubit ( $N_H$ ), and when a qubit is idling during the time Hadamard gates are applied elsewhere ( $N_I$ ).

level, all qubits are subject to independent damping noise

$$\mathcal{L}_{\text{damp}} = \gamma_{\text{damp}} \sum_i \left[ \sigma_i^+ \rho \sigma_i^- - \frac{1}{2} \{ \sigma_i^- \sigma_i^+, \rho \} \right]. \quad (44)$$

We assume  $\gamma_{\text{damp}}$  is measured in (inverse) units of  $t_R$ . Using this information, we can construct an effective noise model for each Hadamard gate, according to the results of Appendix A. Since the single qubit rotations and Ising interactions possess angles that are proportional to the Trotter step size, we can assume that the noise accumulated during their implementation is negligible compared with the noise following a Hadamard gate (for a Trotter step size of  $\tau = 0.1$  and Hamiltonian parameters with unit coupling, the small angle gates possess a gate time approximately 50 times smaller than a Hadamard gate). However, we do account for the noise which accumulates on qubits while other qubits have Hadamard gates applied to them.

In Figure 8 we display the result of performing such a time evolution. Here we take  $J\tau = g\tau = 0.1$ , with a noise strength of  $\gamma_{\text{damp}} t_R = 10^{-4}$ . With our usual definition  $\phi = 2J\tau = 2g\tau$ , notice that this choice ensures

$$\gamma_{\text{damp}} t_R \ll \phi^2 \ll \phi \quad (45)$$

for all relevant gates. Shown is the “exact” time evolution according to the operations and noise terms precisely as they appear in the circuit, as well as a time evolution of the effective model found through our analysis. The strong agreement validates the results of our analysis. Here we choose to display the time evolution of  $\sigma^x$  on the last site, although all observables in the system display a similar level of agreement.

In addition to displaying our effective model, in Figure 9 we see a comparison with several other models which one might assume for the effective noise occurring during the simulation. In particular, we compare our results against models in which we assume that the effective noise is equivalent to independent damping, dephasing, or depolarizing noise. We also show a model in which we assume that noise can be accounted for by simply applying a depolarization channel to the

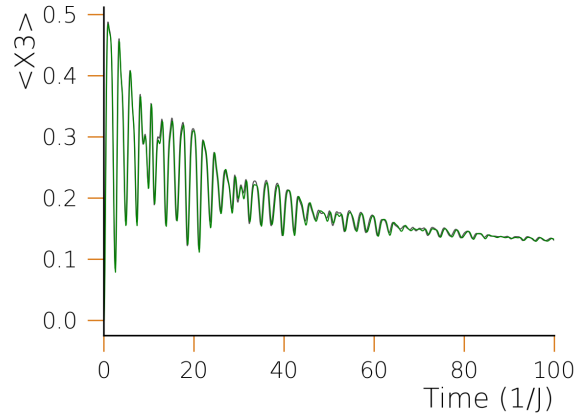


Figure 8: The comparison between the “exact” circuit evolution (green) and the noise mapper output (black).

global density matrix,

$$\rho \rightarrow (1 - \lambda)\rho + \frac{\lambda}{\mathcal{D}} I, \quad (46)$$

which is equivalent to the Lindblad noise

$$\mathcal{L}\{\rho\} = \frac{\gamma_{DC}}{\mathcal{D}^2} \sum_{\alpha} [A_{\alpha} \rho A_{\alpha} - \rho] \quad (47)$$

where the sum is over all products of Pauli operators  $\{A_{\alpha}\}$ , and

$$\lambda \equiv 1 - e^{-\gamma_{DC} t}. \quad (48)$$

In all such cases, the effective models are found by matching the correct overall noise strength to that of the underlying hardware noise. Lastly, we show a comparison to the noise model we would find when failing to account for the effects of commuting noise terms past large gates.

In all such cases, we see very poor agreement with the actual circuit dynamics. Not only are the amplitudes of the curves noticeably different, but the steady states are clearly not in agreement. This motivates the need for the careful noise analysis we have performed in the previous section. Note that for several of the alternative noise models, it would appear as though the qualitative features of the plots are similar, with only deviations in the amplitude being present, and so perhaps the curves could be brought into agreement by adjusting the overall noise strength of the models (rather than simply matching the overall noise strength to that of the underlying hardware noise). However, this in fact does not work - manually adjusting the noise rates in such a way will also lead to a qualitative change in the dynamics, such that when the two curves are made to overlap, the qualitative features no longer agree. Additionally, even if we were to attempt to adjust the overall noise strength in this way, this would not be able to account for the difference in the steady states.



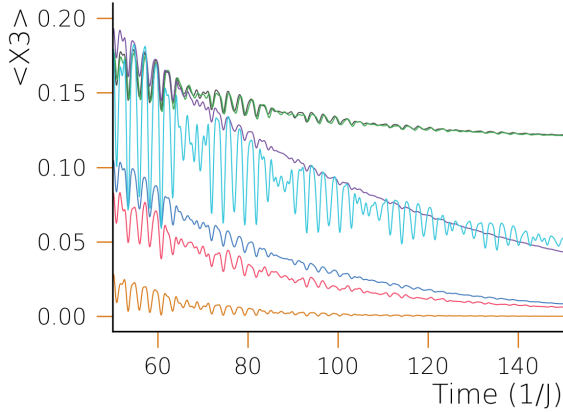


Figure 9: The time evolution, compared against several other potential noise models. The effective noise models which assume independent damping (light blue), dephasing (purple), and depolarizing (dark blue) all show poor agreement with the actual circuit dynamics. The same can be said for the global depolarizing channel (gold), and the effective model in which we neglect the effects of the large gate issue (red). Only the noise model which results from our previous noise analysis (black) shows good agreement with the actual circuit dynamics (green).

## 6 Conclusion

In this work we have presented a method for analyzing the effects of noise in quantum circuits, specifically those which are designed to simulate the time evolution of quantum spin systems through Trotterization. Our method describes the effects of noise through the use of an effective noise model, the *noisy algorithm model*, the time evolution of which provides a good approximation to the actual dynamics of the noisy quantum circuit. While the results presented here have considered the case of time-independent Hamiltonians, the generalization to the time-dependent case is straight-forward.

An obvious generalization of our work would be the extension to Hamiltonians with degrees of freedom other than spins - for example, fermionic degrees of freedom, implemented on a quantum device through the Jordan-Wigner transformation. The philosophy of our analysis, according to which noise terms are shuffled around in a circuit until only small-angle gates and noise terms remain, should still be valid in such a case. The primary consideration, however, would be whether the resulting noise model would have any physical interpretation, after the spin degrees of freedom are transformed back to fermionic degrees of freedom [14]. We leave further investigation of this matter as an open question.

The noisy algorithm model may not only help to understand the extent to which the result of a digital quantum simulation may differ from the intended calculation: Potentially, one could use this framework

to find open quantum systems of interest that may be faithfully simulated on a noisy quantum device. That would be the case, if one tailors the circuit, as well as the noise of the device [24], such that the noisy algorithm model coincides with that open quantum system. Simulating open quantum systems is an active field of research [25–27], hence, offering a new computational tool could be highly beneficial. However, studying this question is out of the scope of this manuscript.

Finally, we hope the results presented in this work will allow for further progress in the field of digital quantum simulation.

## Acknowledgments

This work received funding by the European Union’s Horizon 2020 program number 899561, AVaQus. We thank Eric Dzienkowski, Sebastian Fischetti, and Brayden Ware for helpful discussions.

## A Noise Assumption Rationale

Throughout our work, we have modeled the effects of noise at the circuit level through the use of individual Lindblad noise terms, each associated to a specific gate operation. Here we justify the use of this model.

Our fundamental assumption will be that each quantum gate can be expressed as a sequence of operations on the qubit degrees of freedom, each of which is Markovian,

$$\mathcal{G} = \prod_i \exp\left(t_{\text{op}}^i \mathcal{L}_{\text{op}}^{(i)}\right). \quad (49)$$

In other words, we assume that we can model every gate as a sequence of Hamiltonian operations applied to the qubit degrees of freedom, which may occur while the qubits are coupled to an external bath described by Lindblad dissipation terms,

$$\begin{aligned} \mathcal{L}_{\text{op}}^{(i)} \equiv & \mathcal{L}_h^{(i)} + \mathcal{L}_B^{(i)} \equiv \\ & -i \left[ h^{(i)}, \cdot \right] + \sum_{n,m} \Gamma_{nm}^{B(i)} \left[ A_n(\cdot) A_m^\dagger - \frac{1}{2} \{ A_m^\dagger A_n, (\cdot) \} \right] \end{aligned} \quad (50)$$

This is in contrast with the ideal gate which one might hope to implement in the noise-free case,

$$G = \prod_i \exp\left(t_{\text{op}}^i \mathcal{L}_h^{(i)}\right) \quad (51)$$

An example of such an operation may be a single-qubit rotation around the X-axis, subject to dephasing noise,

$$H = J\sigma^x ; \mathcal{L}_D \{\rho\} = \gamma_{\text{deph}} \sum_i [\sigma_i^z \rho \sigma_i^z - \rho], \quad (52)$$

with some coupling strength  $J$  and dephasing rate  $\gamma_{\text{deph}}$ .

We will assume in all cases that the effects of noise are small compared with the coherent time evolution. For the example above, this would correspond to  $\gamma_{\text{deph}} \ll J$ . We do not, however, make any assumptions about the magnitude of the rotation implemented by the Hamiltonian term - we may have, for example,  $\theta = Jt_{\text{op}} \sim \mathcal{O}(1)$  for a sufficiently large rotation.

While our fundamental assumption will not be valid for all sources of error on all forms of quantum hardware [28–30], describing noise on the device via such Lindblad formalism is well established in the community and proven to be reasonably accurate in practice [22, 31].

We now proceed to demonstrate how, to first order in the noise strength, this fundamental assumption leads to the noise model we have used throughout the main work.

## A.1 Justification Given the Separability Ansatz

We will now proceed to justify the validity of our chosen noise assumptions, given what we refer to as the *separability ansatz*: to lowest order in the noise strength, it is always possible to write

$$\exp\left(t_{\text{op}}^i \mathcal{L}_{\text{op}}^{(i)}\right) \approx \exp\left(t_{\text{op}}^i \mathcal{L}_S^{(i)}\right) \exp\left(t_{\text{op}}^i \mathcal{L}_h^{(i)}\right) \quad (53)$$

where  $\mathcal{L}_h^{(i)}$  is the original noise-free Hamiltonian part, and  $\mathcal{L}_S^{(i)}$  is an effective noise term, which is purely Lindblad, with no Hamiltonian part (the form of this effective noise term may differ significantly from that of the original noise term  $\mathcal{L}_B^{(i)}$ ). In particular, the overall noise strength of  $\mathcal{L}_S^{(i)}$  is the same as  $\mathcal{L}_B^{(i)}$ . We will refer to the term  $\mathcal{L}_S$  as the “separated noise.” We will prove this ansatz shortly - for now, we demonstrate how it leads to our noise model.

With this ansatz, the action of the gate becomes, to lowest order in the noise strength,

$$\mathcal{G} \approx \prod_i \exp\left(t_{\text{op}}^i \mathcal{L}_S^{(i)}\right) \exp\left(t_{\text{op}}^i \mathcal{L}_h^{(i)}\right) \quad (54)$$

Since the gate has now been written as a sequence of pure Hamiltonian and pure Lindblad terms, and since we know from Appendix B the effect of commuting a noise term past a Hamiltonian term, we can commute all of the noise terms to the left, to find

$$\mathcal{G} \approx \prod_i \exp\left(t_{\text{op}}^i \mathcal{L}_N^{(i)}\right) \prod_i \exp\left(t_{\text{op}}^i \mathcal{L}_h^{(i)}\right) \quad (55)$$

where  $\mathcal{L}_N^{(i)}$  is the result of commuting  $\mathcal{L}_S^{(i)}$  past all of the Hamiltonian terms which were originally to its left. Finally, because the underlying noise strength  $\gamma$  is assumed to be appropriately small, and since none of the transformations which lead to  $\mathcal{L}_N^{(i)}$  alter this

noise strength, then all of the terms  $\{\mathcal{L}_N^{(i)}\}$  should themselves be appropriately small. Thus, it is valid to combine all of these noise terms together using the BCH expansion to lowest order, resulting in

$$\mathcal{G} \approx \exp\left(\sum_i t_{\text{op}}^i \mathcal{L}_N^{(i)}\right) \prod_i \exp\left(t_{\text{op}}^i \mathcal{L}_h^{(i)}\right). \quad (56)$$

If we now associate,

$$t_G \mathcal{L}_N^G \equiv \sum_i t_{\text{op}}^i \mathcal{L}_N^{(i)} ; t_G \equiv \sum_i t_{\text{op}}^i \quad (57)$$

then we ultimately find

$$\mathcal{G} \approx \mathcal{N}_G \mathcal{G} \quad (58)$$

We have thus managed to express an arbitrary noisy gate as a clean gate, followed by an individual noise term, as desired.

## A.2 Analysis of the Separated Noise

The justification of our noise model depends on our separability ansatz. Thus, we now discuss the validity of this ansatz. We also discuss various features of the separated noise, and provide some examples.

### A.2.1 A Formal Expression for the Separated Noise

In order to find an expression for the separated noise, we must find a solution to the equation

$$e^{X+Y} = e^W e^X \quad (59)$$

for  $W$  in terms of  $X$  and  $Y$ , under the assumption that  $Y$  is sufficiently “small” in comparison to  $X$ . A recursive formula [32] for the exponentiation of  $W$  can be written

$$e^W = \sum_{m=0}^{\infty} \frac{1}{m!} V_m, \quad (60)$$

where

$$V_0 = I ; V_1 = Y ; V_{m+1} = [X, V_m] + Y V_m \quad (61)$$

When only retaining terms to lowest order in  $Y$ , this recursion relation simplifies to

$$V_0 = I ; V_{m \neq 0} = \Lambda^{(m-1)}(Y), \quad (62)$$

where

$$\Lambda(Y) \equiv [X, Y] \quad (63)$$

such that  $\Lambda^{(m-1)}$  is the  $(m-1)$  times nested commutator under  $X$ . We can thus write

$$e^W = I + \sum_{m=1}^{\infty} \frac{1}{m!} \Lambda^{(m-1)}(Y), \quad (64)$$

or, alternatively,

$$e^W = I + \sum_{m=0}^{\infty} \frac{1}{(m+1)!} \Lambda^m(Y). \quad (65)$$

Now, assuming that  $W$  has some expansion in powers of the overall noise strength, we can write

$$W = w_0 + \gamma w_1 + \gamma^2 w_2 + \dots \quad (66)$$

where  $\gamma$  is the overall scale of  $Y$ . From the original defining equation, it is clear that when  $Y$  vanishes, such that  $\gamma = 0$ , we must have

$$\begin{aligned} e^X = e^W e^X &\Rightarrow e^W = I = e^0 \Rightarrow \\ W(\gamma = 0) = 0 &\Rightarrow w_0 = 0 \end{aligned} \quad (67)$$

Thus,  $W$  itself must already be of order  $\gamma$ . Thus, we find that

$$\begin{aligned} e^W &\approx I + W + \frac{1}{2}W^2 + \dots \\ &\approx I + (\gamma w_1 + \gamma^2 w_2 + \dots) + \frac{1}{2}(\gamma w_1 + \gamma^2 w_2 + \dots)^2 + \dots \\ &\approx I + \gamma w_1 + \dots \end{aligned} \quad (68)$$

Comparing the two expressions we have found for the exponentiation of  $W$  to first order in the noise strength, we see that we can make the association

$$\gamma w_1 \rightarrow \sum_{m=0}^{\infty} \frac{1}{(m+1)!} \Lambda^m(Y), \quad (69)$$

which, to lowest order in the noise strength, implies

$$W \approx \sum_{m=0}^{\infty} \frac{1}{(m+1)!} \Lambda^m(Y). \quad (70)$$

Summing this series, we find the closed-form expression,

$$f(x) = \sum_{m=0}^{\infty} \frac{x^m}{(m+1)!} = \frac{e^x - 1}{x}, \quad (71)$$

which allows us to write

$$W = \mathcal{F}_\Lambda[Y] ; \mathcal{F}_\Lambda \equiv \frac{e^\Lambda - \mathcal{I}}{\Lambda}. \quad (72)$$

where  $\mathcal{I}$  is the identity map,

$$\mathcal{I}[Y] = Y. \quad (73)$$

Using this result, we can now return to our original problem of finding an expression for the separated noise, which yields

$$\mathcal{L}_S = \mathcal{F}_\Lambda[\mathcal{L}_B], \quad (74)$$

with

$$\Lambda(\mathcal{L}_B) = t_{\text{op}}[\mathcal{L}_h, \mathcal{L}_B] \quad (75)$$

We have thus found an explicit expression for  $\mathcal{L}_S$  to first order in the noise strength. We now proceed to argue that, somewhat remarkably,  $\mathcal{L}_S$  is itself a term of pure Lindblad form, which is in fact physical (its underlying rate matrix is positive semi-definite).

## A.2.2 The Rate Matrix of the Separated Noise

To demonstrate that  $\mathcal{L}_S$  can be expressed as a super-operator written in standard Lindblad form, we begin by explicitly computing the action

$$\Lambda(\mathcal{L}_B)\{\rho\} = t_{\text{op}}[\mathcal{L}_h \mathcal{L}_B - \mathcal{L}_B \mathcal{L}_h]\{\rho\} \quad (76)$$

for some arbitrary density matrix  $\rho$ . Evaluating this expression and performing some minor algebraic rearrangement, we ultimately find

$$\begin{aligned} \Lambda(\mathcal{L}_B) = t_{\text{op}} \sum_{n,m} \Gamma_{nm}^B &\left[ Z_n \rho A_m^\dagger - \frac{1}{2} \{A_m^\dagger Z_n, \rho\} \right. \\ &\left. + A_n \rho Z_m^\dagger - \frac{1}{2} \{Z_m^\dagger A_n, \rho\} \right], \end{aligned} \quad (77)$$

where we have defined

$$Z_n \equiv -i[h, A_n]. \quad (78)$$

From here, for simplicity, we will assume that the basis of generators  $\{A_n\}$  is Hermitian - it is always possible to choose our basis in this way, without loss of generality (an example of such a choice would be the generators of  $su(\mathcal{D})$  in the defining representation, or the set of all Pauli operator products on  $n$  qubits). Expanding the Hamiltonian term in this basis, we have

$$h = \sum_i \alpha_i^{(h)} A_i, \quad (79)$$

for some set of real coefficients  $\{\alpha_i^{(h)}\}$  (any component of the Hamiltonian along the identity can be neglected, since this will not have any effect on the transformation). With this definition, we find

$$Z_n = -i \left[ \sum_i \alpha_i^{(h)} A_i, A_n \right] = \sum_{i,j} \alpha_i^{(h)} f_{inj} A_j, \quad (80)$$

where the  $\{f_{inj}\}$  are the (real) structure constants of the algebra generated by the  $\{A_n\}$ ,

$$[A_i, A_n] = +i \sum_j f_{inj} A_j \quad (81)$$

Inserting the above expression for  $Z_n$  into the previously found expression for  $\Lambda(\mathcal{L}_B)$ , and performing some minor simplification and relabeling of indices, we find

$$\Lambda(\mathcal{L}_B) = \sum_{n,m} \left( \phi^{(h)}[\Gamma^B] \right)_{nm} \left[ A_n \rho A_m^\dagger - \frac{1}{2} \{A_m^\dagger A_n, \rho\} \right] \quad (82)$$

where we have defined,

$$\left( \phi^{(h)}[\Gamma^B] \right)_{nm} = t_{\text{op}} \sum_{i,j} \alpha_i^{(h)} (f_{ijn} \Gamma_{jm}^B + f_{ijm} \Gamma_{nj}^B) \quad (83)$$

This can alternately be written as

$$\begin{aligned} \left(\phi^{(h)}[\Gamma^B]\right)_{nm} &= \sum_{ij} \Phi_{nm,ij}^{(h)} \Gamma_{ij}^B; \\ \Phi_{nm,ij}^{(h)} &\equiv t_{\text{op}} \sum_p \alpha_p^{(h)} (f_{pin} \delta_{jm} + f_{pjm} \delta_{in}). \end{aligned} \quad (84)$$

We thus see that the action  $\Lambda(\mathcal{L}_B)$  corresponds to an object which superficially takes the form of a Lindblad noise term. Likewise, since we have now found that commuting a Hamiltonian super-operator with a Lindblad noise term produces another Lindblad noise term, the same must hold true for any higher-order nested commutators under the action of  $\mathcal{L}_h$ ,

$$\Lambda^m(\mathcal{L}_B) = [t_{\text{op}} \mathcal{L}_h, [t_{\text{op}} \mathcal{L}_h, \dots [t_{\text{op}} \mathcal{L}_h, \mathcal{L}_B] \dots]] \quad (85)$$

Therefore, the full expression for the transformed noise,

$$\mathcal{L}_S = \mathcal{F}_\Lambda[\mathcal{L}_B] = \sum_{m=0}^{\infty} \frac{1}{(m+1)!} \Lambda^m(\mathcal{L}_B) \quad (86)$$

must likewise correspond to a term of Lindblad form, since the sum of two Lindblad terms is another Lindblad term. It is clear that the transformation of the underlying rate matrix under such a nested commutator is found via the corresponding composition of the map  $\phi$ ,

$$\mathcal{L}'_B = \Lambda^m(\mathcal{L}_B) \Rightarrow \Gamma^{B'} = \phi^m(\Gamma^B), \quad (87)$$

where we have dropped the superscript on  $\phi$  for the sake of simplicity.

Furthermore, since Lindblad terms are in one-to-one correspondence with their rate matrices (assuming we have fixed a specific basis for the  $\{A_n\}$ ), and since adding two noise terms corresponds to directly adding their corresponding rate matrices, we can more naturally interpret the full transformation  $\mathcal{F}$  as acting rather on the underlying rate matrix of  $\mathcal{L}_B$ , such that

$$\Gamma^S = \mathcal{F}_\phi[\Gamma^B] \equiv \sum_{m=0}^{\infty} \frac{1}{(m+1)!} \phi^m(\Gamma^B). \quad (88)$$

In other words, we have the equivalence

$$\mathcal{L}_S = \mathcal{F}_\Lambda[\mathcal{L}_B] \Leftrightarrow \Gamma^S = \mathcal{F}_\phi[\Gamma^B] \quad (89)$$

We point out here two important properties of the maps  $\phi$  and  $\mathcal{F}_\phi$ . First, using the anti-symmetry of the structure constants, it is easy to verify that the map  $\phi$ , and therefore also the map  $\mathcal{F}_\phi$ , preserve the Hermitian nature of the rate matrix. Second, again making use of the anti-symmetry of the structure constants, we find

$$\text{Tr}[\phi(\Gamma)] = 0 \quad (90)$$

for any  $\Gamma$ , and thus

$$\gamma^S = \text{Tr}[\Gamma^S] = \text{Tr}[\mathcal{F}_\phi[\Gamma^B]] = \text{Tr}[\Gamma^B] = \gamma^B. \quad (91)$$

Thus the map  $\mathcal{F}_\phi$  preserves the overall noise scale.

### A.2.3 The Physical Nature of the Separated Noise

We have found that the separated noise

$$\mathcal{L}_S = \mathcal{F}_\Lambda[\mathcal{L}_B] \quad (92)$$

superficially takes the form of a Lindblad dissipator, with an underlying rate matrix given according to

$$\Gamma^S = \mathcal{F}_\phi[\Gamma^B] \quad (93)$$

In order to demonstrate that this term is physical, we must show that the matrix  $\Gamma^S$  is positive semi-definite, so long as  $\Gamma^B$  is positive semi-definite. In other words, we must demonstrate that the map  $\mathcal{F}_\phi$  is a positive map. In fact, we have found that for all relevant cases of interest,  $\mathcal{F}_\phi$  is not only positive, but rather completely positive (and is therefore in fact a CPTP map). Proving such a claim can be done by demonstrating that the associated Choi matrix of the map is positive, where the Choi matrix is defined according to

$$C_{\mathcal{F}} = \sum_{i,j} e^{ij} \otimes \mathcal{F}_\phi[e^{ij}], \quad (94)$$

where  $e^{ij}$  is the matrix with  $(i, j)$  entry equal to one, with zeros elsewhere.

While proving the positivity of this object in the general case is a formidable task, it is a relatively straight-forward exercise to compute this matrix numerically, for specific choices of the Hamiltonian term  $\mathcal{L}_h$ . Having done so for all single-qubit and pair-interaction Hamiltonian terms, we have found the Choi matrix to possess a positive spectrum in all such cases. Since we assume that the operations  $\mathcal{L}_{\text{op}}^{(i)}$  composing a quantum gate are likely to consist of one and two-body interaction terms, this guarantees the physical nature of the separated noise  $\mathcal{L}_S$  in all relevant cases of interest.

In fact, for the case of a single-qubit term, it is possible to derive an analytic expression for the Choi matrix, which we demonstrate here as an example. Let us consider an operation with

$$\begin{aligned} \mathcal{L}_{\text{op}}(\rho) &= \mathcal{L}_h(\rho) + \mathcal{L}_B(\rho) = \\ &-i[h, \rho] + \sum_{\alpha, \beta} \Gamma_{\alpha\beta}^B \left[ \sigma^\alpha \rho \sigma^\beta - \frac{1}{2} \{ \sigma^\beta \sigma^\alpha, \rho \} \right], \end{aligned} \quad (95)$$

where the  $\{\sigma^\alpha\}$  are the usual Pauli operators acting on a single qubit. Here we choose to take

$$h = -\sigma^x. \quad (96)$$

Any other choice of Hamiltonian is equivalent through rotational symmetry and resealing of units. The rate matrix in this case is a  $3 \times 3$  positive semi-definite matrix,

$$\Gamma^B \rightarrow \begin{bmatrix} \Gamma_{XX}^B & \Gamma_{XY}^B & \Gamma_{XZ}^B \\ \Gamma_{YX}^B & \Gamma_{YY}^B & \Gamma_{YZ}^B \\ \Gamma_{ZX}^B & \Gamma_{ZY}^B & \Gamma_{ZZ}^B \end{bmatrix} \quad (97)$$

The matrix  $\Phi$  is given according to

$$\Phi_{nm,ij} = -t_{\text{op}} (\epsilon_{Xin}\delta_{jm} + \epsilon_{Xjm}\delta_{in}), \quad (98)$$

where the structure constants are given simply by the Levi-Civita symbol. It is easy to verify that this matrix is anti-symmetric and real, and hence anti-Hermitian (this is in fact generally true, as can be seen from the original definition). In this case, the only non-zero elements of the transformation are given

$$\begin{aligned} \Phi_{XY,XZ} = \Phi_{YX,ZX} = \Phi_{YY,YZ} = \Phi_{YY,ZY} \\ = \Phi_{YZ,ZZ} = \Phi_{ZY,ZZ} = +t_{\text{op}}, \end{aligned} \quad (99)$$

along with the corresponding entries related to these by anti-symmetry.

In order to compute the full transformation  $\mathcal{F}_\phi$  as a matrix acting on the space of rate matrices, it is easiest to diagonalize the matrix  $\Phi$ , compute the function  $f$  on this diagonal matrix, and rotate back to the original basis (such a diagonalization is always guaranteed, due to the anti-Hermitian structure of  $\Phi$ ). In this case,  $\Phi$  is a  $9 \times 9$  matrix, and its spectrum can be computed in closed form, using symbolic manipulation software such as Wolfram Mathematica. While its form is not particularly illuminating, and is too cumbersome to reproduce here, its entries consist of relatively simple trigonometric functions of the time  $t_{\text{op}}$ .

Once we have constructed the map  $\mathcal{F}_\phi$ , we can build the Choi matrix of the map, which is again a  $9 \times 9$  matrix, constructed according to the definition above. Again, while the full Choi matrix is too cumbersome to reproduce in its entirety here, its entries consist of relatively simple trigonometric functions of  $t_{\text{op}}$ . Much more interesting is the spectrum of the Choi matrix, which can, somewhat miraculously, be computed in closed form. The Choi matrix in this case possesses three non-zero eigenvalues, which are given according to

$$\begin{aligned} \lambda_0 &= 1 - \frac{\sin(t_{\text{op}})}{t_{\text{op}}}; \\ \lambda_{\pm} &= 1 + \frac{\pm\sqrt{2\cos(t_{\text{op}}) + 34}\sin\left(\frac{t_{\text{op}}}{2}\right) + \sin(t_{\text{op}})}{2t_{\text{op}}} \end{aligned} \quad (100)$$

A plot of this spectrum is shown in Figure 10. The positive nature of the spectrum demonstrates explicitly that the map  $\mathcal{F}_\phi$  is a positive map in the single-qubit case.

While the form of the Choi matrix does not lend itself to an analytic expression for the case of two-qubit Hamiltonian interactions, it is still possible to evaluate the spectrum of the Choi matrix numerically in such cases. As mentioned previously, we have found the map to be positive for all two-qubit pair interaction terms.

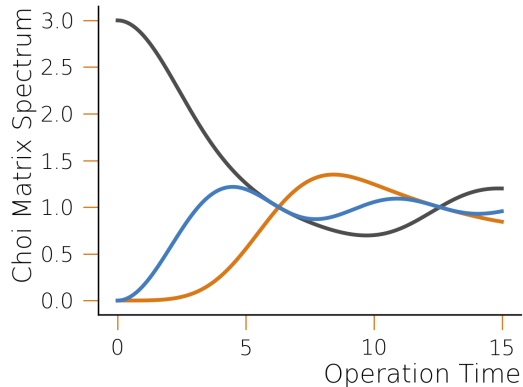


Figure 10: The spectrum of the Choi matrix for the single-qubit case, as a function of the operation time  $t_{\text{op}}$ . Note that in this case, a time  $t_{\text{op}} = \pi$  already corresponds to a  $2\pi$  rotation around the  $x$ -axis, and thus times larger than this are likely to be irrelevant in most practical cases of interest.

#### A.2.4 Examples of Separated Noise

In the single-qubit case, it is possible to evaluate the transformation of the noise explicitly. Here we provide a few examples, using the same Hamiltonian term, and hence the same transformation  $\phi$ , as above.

For dephasing noise on a single qubit, the rate matrix is

$$\Gamma^B \rightarrow \gamma \begin{bmatrix} 0 & 0 & 0 \\ 0 & 0 & 0 \\ 0 & 0 & 1 \end{bmatrix} \quad (101)$$

where  $\gamma$  is the dephasing rate, also equal to the overall noise strength. Applying the transformation to this matrix, we find

$$\Gamma^S \rightarrow \frac{\gamma}{2t} \begin{bmatrix} 0 & 0 & 0 \\ 0 & t - \cos(t)\sin(t) & \sin^2(t) \\ 0 & \sin^2(t) & t + \cos(t)\sin(t) \end{bmatrix} \quad (102)$$

For notational simplicity we drop the subscript on  $t_{\text{op}}$ ; all times discussed here are understood to be the time required to implement a single operation, several of which may constitute a single gate. Note in this case we can see explicitly how the trace and Hermitian nature of the rate matrix are preserved. It is also quite clear that for general values of the parameter  $t_{\text{op}}$ , the noise can deviate quite significantly in nature from its original form. The non-zero eigenvalues of this transformed matrix represent the noise rates, of which there are two,

$$\gamma_{\pm} = \frac{1}{2} \left( 1 \pm \frac{\sin(t)}{t} \right) \quad (103)$$

A plot of these eigenvalues as a function of the parameter  $t$  is shown in Figure 11. We see explicitly how the positivity of the spectrum is preserved by the transformation.

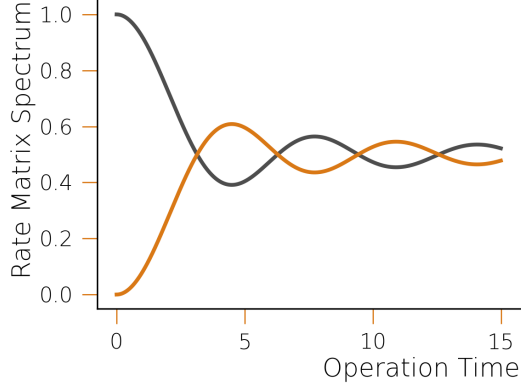


Figure 11: The transformed dephasing spectrum, as a function of operation time.

Another important example of single qubit noise is damping noise, given by

$$\Gamma^B \rightarrow \frac{\gamma_{\text{damp}}}{4} \begin{bmatrix} 1 & -i & 0 \\ +i & 1 & 0 \\ 0 & 0 & 0 \end{bmatrix} \quad (104)$$

In this case, the transformed noise is somewhat more complicated,

$$\Gamma^S \rightarrow \frac{\gamma_{\text{damp}}}{8t} \times \begin{bmatrix} 2t & -2i \sin(t) & -2i (\cos(t) - 1) \\ 2i \sin(t) & t + \sin(t) \cos(t) & -\sin^2(t) \\ 2i (\cos(t) - 1) & -\sin^2(t) & t - \sin(t) \cos(t) \end{bmatrix} \quad (105)$$

Likewise, the spectrum of this rate matrix is now correspondingly more complicated, with three non-zero noise rates given by

$$\begin{aligned} \gamma_0 &= \frac{1}{8} \left( 1 - \frac{\sin(t)}{t} \right); \\ \gamma_{\pm} &= \frac{3}{16} + \frac{1}{32t} \left[ 2 \sin(t) \right. \\ &\quad \left. \pm \sqrt{2\sqrt{2t^2 - 4t \sin(t) - 64 \cos(t) - \cos(2t)} + 65} \right] \end{aligned} \quad (106)$$

Again, a plot of this spectrum is shown in Figure 12.

Lastly, we consider depolarizing noise acting on a single qubit. In this case, the rate matrix is proportional to the identity matrix  $\delta$ , and we in fact have

$$\phi(\delta) = 0 \Rightarrow \mathcal{F}_\phi[\delta] = \delta. \quad (107)$$

Thus, depolarizing noise possesses the property that it can be separated without any change to its structure. This is merely a reflection of the fact that depolarizing noise commutes with any coherent dynamics, and thus separating the exponential terms in this case is exact.

In the two-qubit case, the rate matrix has dimensions  $15 \times 15$ , and the structure of the map  $\mathcal{F}_\phi$  becomes

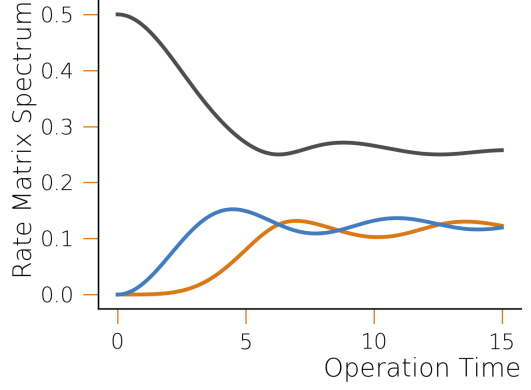


Figure 12: The transformed damping spectrum, as a function of operation time.

significantly more complicated. We do not attempt an analytic evaluation of the map in this case, however, it is of course always possible to perform the transformation numerically. One important feature of the two-qubit case which we mention here, is that the transformation  $\mathcal{F}_\phi$  can produce correlated noise from uncorrelated noise. For example, in the case that the Hamiltonian represents a pair interaction, and the original noise corresponds to independent dephasing (a case which will be considered in more detail shortly), the separated noise contains contributions which involve correlations among both qubits.

#### A.2.5 Accuracy of the separated time evolution

We have argued above that, to first order in the noise strength, it is always possible to approximate

$$e^{t_{\text{op}}^i \mathcal{L}_h^{(i)} + t_{\text{op}}^i \mathcal{L}_B^{(i)}} \approx e^{t_{\text{op}}^i \mathcal{L}_S^{(i)}} e^{t_{\text{op}}^i \mathcal{L}_h^{(i)}}. \quad (108)$$

We would now like to demonstrate the accuracy of this assumption. To this end, we will study the case of independent dephasing noise on two qubits, subject to a pair-X interaction,

$$\mathcal{L}_{\text{op}}\{\rho\} = -i[-\sigma_a^x \sigma_b^x, \rho] + \gamma_{\text{deph}} \sum_i [\sigma_i^z \rho \sigma_i^z - \rho]. \quad (109)$$

Of interest to us will be the original time-evolution, compared with the time-evolution under our separated approximation. We will also compare against the case in which the noise is separated from the coherent part without the appropriate transformation,

$$e^{t_{\text{op}}^i \mathcal{L}_h^{(i)} + t_{\text{op}}^i \mathcal{L}_B^{(i)}} \rightarrow e^{t_{\text{op}}^i \mathcal{L}_B^{(i)}} e^{t_{\text{op}}^i \mathcal{L}_h^{(i)}}, \quad (110)$$

as well as the case where we have neglected the noise entirely,

$$e^{t_{\text{op}}^i \mathcal{L}_h^{(i)} + t_{\text{op}}^i \mathcal{L}_B^{(i)}} \rightarrow e^{t_{\text{op}}^i \mathcal{L}_h^{(i)}}. \quad (111)$$

Figure 13 demonstrates the accuracy of our noise assumptions. We have chosen to display here the

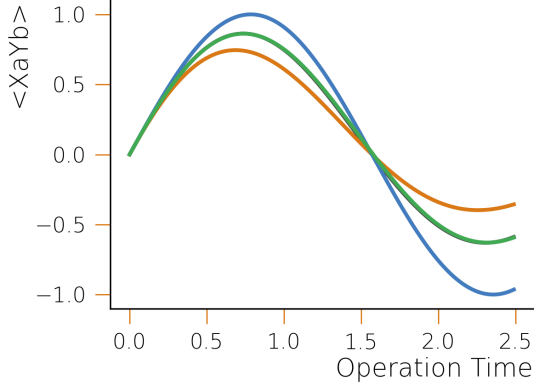


Figure 13: The time evolution of the observable  $\sigma_a^x \sigma_b^y$ , according to the exact dynamics (green) and our approximate model for the separated noise (black). These two curves are almost indistinguishable. We also display the time evolution under the assumption that we can simply split apart the noise with no modification (orange), as well as the time evolution in the case that there is no noise at all (blue).

time evolution of the observable  $\sigma_a^x \sigma_b^y$ , starting from the initial state in which both spins are polarized up along the z-axis. We see that our effective noise model is an exceptionally good approximation to the original time evolution, even for noise strengths as large as  $\gamma = 0.1$ . Furthermore, we see that this agreement is not merely a result of the noise term being unimportant - the poor agreement with the other two approximations demonstrates that the effects of noise are indeed important, and that care must be taken to implement the noise separation correctly. While we have displayed here one particular choice of observable, we have found the same exceptional agreement for all choices of observable and initial state (although for some observables, the other two approximations are valid as well, indicating that not every observable is affected equally by the presence of noise).

### A.3 Example of Gate Noise

To conclude, we present here an example of a noise term following a gate, according to our above analysis. We assume a toy model of an ideal Hadamard gate,

$$U_H = R_y(\pi/2)Z = \exp(-i\frac{\pi}{4}Y) \exp(-i\frac{\pi}{2}(I - Z)). \quad (112)$$

Since an overall phase is not measurable in practice, we study simply

$$U_H \rightarrow \exp(-i\frac{\pi}{4}Y) \exp(+i\frac{\pi}{2}Z). \quad (113)$$

Furthermore, we assume that there is hardware noise occurring during the implementation of this gate, which in this case we take to be damping noise,

$$\mathcal{L}_{\text{damp}} = \gamma_{\text{damp}} \left[ \sigma^+ \rho \sigma^- - \frac{1}{2} \{ \sigma^- \sigma^+, \rho \} \right] \quad (114)$$

In order to determine the effective noise term following this gate, we must first determine the separated noise, then commute all noise terms to the left, and finally sum up the commuted noise.

To begin, we must compute the separated noise for each part. We write the Liouvillian of the first operation as

$$\mathcal{L}_{\text{op}}^Z \{ \rho \} = -iJ_Z [\sigma^z, \rho] + \gamma_{\text{damp}} \left[ \sigma^+ \rho \sigma^- - \frac{1}{2} \{ \sigma^- \sigma^+, \rho \} \right] \quad (115)$$

From the definition of our toy model, we see that we must take

$$J_Z t_{\text{op}}^Z = -\pi/2 \quad (116)$$

We will choose to define the quantity  $t_R$  as the time required to implement a rotation of  $\pi/2$ , which we assume is the same for both operations. With this definition, we find

$$t_{\text{op}}^Z = 2t_R; \quad J_Z = -\frac{\pi}{4} t_R^{-1} \quad (117)$$

We further assume that  $\gamma_{\text{damp}}$  is measured in units of  $t_R^{-1}$ ; its precise value will of course depend on the degree of noise present on the chosen hardware. For the second operation, we similarly write

$$\mathcal{L}_{\text{op}}^Y \{ \rho \} = -iJ_Y [\sigma^y, \rho] + \gamma_{\text{damp}} \left[ \sigma^+ \rho \sigma^- - \frac{1}{2} \{ \sigma^- \sigma^+, \rho \} \right] \quad (118)$$

with

$$t_{\text{op}}^Y = t_R; \quad J_Y = \frac{\pi}{4} t_R^{-1} \quad (119)$$

In order to compute the separated noise, we must again compute the transformation  $\phi$  on the underlying rate matrix. For the first operation, the noise remains unchanged after separation, since damping noise commutes with a Hamiltonian proportional to  $\sigma^z$ , and thus

$$\Gamma_Z^S \rightarrow \gamma_{\text{damp}} \begin{bmatrix} \frac{1}{4} & -\frac{i}{4} & 0 \\ \frac{i}{4} & \frac{1}{4} & 0 \\ 0 & 0 & 0 \end{bmatrix} \quad (120)$$

For the second transformation, we can follow a procedure similar to that of the previous examples. Applying the transformation  $\mathcal{F}_\phi$  to the damping rate matrix, and enforcing  $t_{\text{op}}^Y J_Y = \pi/4$ , we find that the separated noise for the second operation is

$$\Gamma_Y^S \rightarrow \gamma_{\text{damp}} \begin{bmatrix} \frac{2+\pi}{8\pi} & -\frac{i}{\sqrt{2}\pi} & -\frac{1}{4\pi} \\ \frac{i}{\sqrt{2}\pi} & \frac{1}{4} & \frac{i(\frac{1}{\sqrt{2}}-1)}{\pi} \\ -\frac{1}{4\pi} & -\frac{i(\frac{1}{\sqrt{2}}-1)}{\pi} & \frac{\pi-2}{8\pi} \end{bmatrix} \quad (121)$$

Having found the separated noise for each operation, we must now commute all of the noise terms to

the left of the coherent terms. For the second operation this is unnecessary, since it is already to the left of all coherent terms. Thus, for the second operation,

$$\Gamma_Y^N \rightarrow \gamma_{\text{damp}} \begin{bmatrix} \frac{2+\pi}{8\pi} & -\frac{i}{\sqrt{2}\pi} & -\frac{1}{4\pi} \\ \frac{i}{\sqrt{2}\pi} & \frac{1}{4} & \frac{i(\frac{1}{\sqrt{2}}-1)}{\pi} \\ -\frac{1}{4\pi} & -\frac{i(\frac{1}{\sqrt{2}}-1)}{\pi} & \frac{\pi-2}{8\pi} \end{bmatrix} \quad (122)$$

For the first operation, we must move the separated noise past the coherent piece of the second operation (the rotation around the y axis). Using the transformation found in Appendix B, we find that the separated noise, after being commuted past the coherent gate, is

$$\Gamma_Z^N \rightarrow \gamma_{\text{damp}} \begin{bmatrix} 0 & 0 & 0 \\ 0 & \frac{1}{4} & -\frac{i}{4} \\ 0 & \frac{i}{4} & \frac{1}{4} \end{bmatrix} \quad (123)$$

Notice that the noise has essentially been “rotated” around the y axis.

Now that all of the noise terms have been commuted to the left, we can add them together to zero order in the BCH formula,

$$t_G \mathcal{L}_N = t_{\text{op}}^Z \mathcal{L}_N^Z + t_{\text{op}}^Y \mathcal{L}_N^Y \quad (124)$$

If we associate

$$t_G = 3t_R \quad (125)$$

and write this in terms of the corresponding rate matrices, we find

$$\Gamma^N = \frac{2}{3}\Gamma_Z^N + \frac{1}{3}\Gamma_Y^N \quad (126)$$

Explicitly, this is

$$\Gamma^N \rightarrow \gamma_{\text{damp}} \begin{bmatrix} \frac{2+\pi}{24\pi} & -\frac{i}{3\sqrt{2}\pi} & -\frac{1}{12\pi} \\ \frac{i}{3\sqrt{2}\pi} & \frac{1}{4} & \frac{i(-2+\sqrt{2}-\pi)}{6\pi} \\ -\frac{1}{12\pi} & \frac{i(2-\sqrt{2}+\pi)}{6\pi} & \frac{1}{24} \left(5 - \frac{2}{\pi}\right) \end{bmatrix} \quad (127)$$

or

$$\Gamma^N \approx \gamma_{\text{damp}} \begin{bmatrix} 0.068 & -0.075i & -0.027 \\ 0.075i & 0.25 & -0.198i \\ -0.027 & 0.198i & 0.182 \end{bmatrix} \quad (128)$$

We thus see that despite the relatively simple nature of both the underlying noise and the gate, the effective noise term can take a relatively complex form.

## B Noise Modification Resulting from Large Gates

In the main text, we have found that in order to analyze circuits which contain “large gate decomposition blocks” (LGDBs), it is necessary to understand how a noise term is modified when it is commuted past a

unitary gate. More concretely, we would like to solve the following equation,

$$e^{\mathcal{L}_G} e^{\mathcal{L}_N} = e^{\mathcal{L}_P} e^{\mathcal{L}_G}, \quad (129)$$

where  $\mathcal{L}_G$  describes the action of a noise-free gate,  $\mathcal{L}_N$  describes the original noise term, and  $\mathcal{L}_P$  describes the modified noise term we wish to find. Formally, the solution to this equation is

$$\mathcal{L}_P = e^{\text{ad}_{\mathcal{L}_G}} \mathcal{L}_N = e^{\mathcal{L}_G} \mathcal{L}_N e^{-\mathcal{L}_G}, \quad (130)$$

which involves the adjoint action of  $\mathcal{L}_G$  on  $\mathcal{L}_N$ .

To evaluate this expression, we note that the superoperator  $\mathcal{L}_G$  corresponds to some unitary gate operation on the density matrix,

$$e^{\mathcal{L}_G} \rho = U_G \rho U_G^\dagger; \quad e^{-\mathcal{L}_G} \rho = U_G^\dagger \rho U_G. \quad (131)$$

Therefore, if we have

$$\mathcal{L}_N \{\rho\} = \sum_{n,m} \Gamma_{nm}^N \left[ A_n \rho A_m^\dagger - \frac{1}{2} \{A_m^\dagger A_n, \rho\} \right], \quad (132)$$

then composing all three operations together, we find

$$\begin{aligned} \mathcal{L}_P \{\rho\} &= e^{\mathcal{L}_G} \{ \mathcal{L}_N \{ e^{-\mathcal{L}_G} \{\rho\} \} \} = \\ &U_G \left[ \sum_{n,m} \Gamma_{nm}^N \left[ A_n \left( U_G^\dagger \rho U_G \right) A_m^\dagger \right. \right. \\ &\left. \left. - \frac{1}{2} \{ A_m^\dagger A_n, \left( U_G^\dagger \rho U_G \right) \} \right] \right] U_G^\dagger. \end{aligned} \quad (133)$$

A straight-forward manipulation of this equation brings it into the alternate form,

$$\begin{aligned} \mathcal{L}_P \{\rho\} &= \\ &\sum_{n,m} \Gamma_{nm}^N \left[ \left( U_G A_n U_G^\dagger \right) \rho \left( U_G A_m U_G^\dagger \right)^\dagger - \right. \\ &\left. \frac{1}{2} \left\{ \left( U_G A_m U_G^\dagger \right)^\dagger \left( U_G A_n U_G^\dagger \right), \rho \right\} \right] \end{aligned} \quad (134)$$

Hence, we see that commuting the noise term past the large gate produces another term of Lindblad form, in which the underlying rate matrix remains the same, but the basis of operators  $\{A_n\}$  has been modified according to

$$A_n \rightarrow E_n \equiv U_G A_n U_G^\dagger = e^{\mathcal{L}_G} A_n \quad (135)$$

The basis  $\{E_n\}$  remains a complete basis of traceless operators under this transformation, and hence  $\mathcal{L}_P$  remains a valid noise term. Noise terms which must be commuted past multiple large gate terms simply pick up a contribution from each large gate that they pass,

$$A_n \rightarrow E_n = U A_n U^\dagger; \quad U \equiv \prod_g U_g. \quad (136)$$



In some cases, rather than viewing this transformation of the noise term as a modification of the basis  $\{A_n\}$ , it might be easier to analyze the modification as a transformation of its underlying rate matrix. To this end, we make use of the fact that the  $\{A_n\}$  constitute a complete basis of all traceless operators, and write

$$E_n = U A_n U^\dagger \equiv \sum_p M_{pn} A_p \quad (137)$$

Inserting this definition into the transformed Lindblad equation, we find

$$\begin{aligned} \mathcal{L}_P \{\rho\} = & \\ \sum_{n,m,p,q} \Gamma_{nm}^N M_{pn} M_{qm} & \left[ A_p \rho A_q^\dagger - \frac{1}{2} \{A_q^\dagger A_p, \rho\} \right]. \end{aligned} \quad (138)$$

Making the identification,

$$\Gamma_{pq}^P \equiv \sum_{n,m} \Gamma_{nm}^N M_{pn} M_{qm} = (M \Gamma^N M^\dagger)_{pq}, \quad (139)$$

we can write

$$\mathcal{L}_P \{\rho\} = \sum_{p,q} \Gamma_{pq}^P \left[ A_p \rho A_q^\dagger - \frac{1}{2} \{A_q^\dagger A_p, \rho\} \right]. \quad (140)$$

We thus find that we can interpret the modification of the noise term as a transformation of its underlying rate matrix, according to

$$\Gamma^N \rightarrow \Gamma^P \equiv M \Gamma^N M^\dagger \quad (141)$$

In order to find an expression for the matrix  $M$ , we take the Hilbert-Schmidt inner product of both sides of the equation defining  $M$  with the operator  $A_m$ , thus finding

$$\text{Tr} [A_m^\dagger U A_n U^\dagger] = \sum_p M_{pn} \text{Tr} [A_m^\dagger A_p]. \quad (142)$$

Defining,

$$\eta_{mp} = \langle \langle A_m || A_p \rangle \rangle \equiv \text{Tr} [A_m^\dagger A_p], \quad (143)$$

we can write

$$\text{Tr} [A_m^\dagger U A_n U^\dagger] = \sum_p \eta_{mp} M_{pn} = (\eta M)_{mn}. \quad (144)$$

Since the  $\{A_n\}$  constitute a complete basis, we can invert the matrix  $g$  to find,

$$M = \eta^{-1} \chi; \quad \chi_{mn} \equiv \text{Tr} [A_m^\dagger U A_n U^\dagger] \quad (145)$$

We note that when the  $\{A_n\}$  are chosen to be a basis of Pauli operators which are normalized according to

$$\eta_{mp} = \text{Tr} [A_m^\dagger A_p] = \delta_{mn}, \quad (146)$$

then we have simply

$$M = \chi. \quad (147)$$

It is a straightforward exercise to verify that the matrix  $M$  is unitary, and for this reason, the noise spectrum of  $\mathcal{L}_N$  is in fact preserved under this transformation (this of course also guarantees that the resulting noise term is physical in nature, assuming that the original noise term was physical).

## C Software Implementation Details

In this appendix, we explain in more detail how we implemented the software to calculate the effective Lindbladian of a noisy quantum algorithm. The tool is built upon *qoqo* [33], the HQS Quantum Simulations package for representing quantum circuits and programs, with backend options for running them on quantum devices, but also a simulator backend for conventional hardware relying on QuEST [34].

In *qoqo*, we have the particular freedom to define on the circuit level any kind of Lindblad noise acting during the application of the quantum program. Hence, we can produce generic noisy quantum algorithms that conform with our noise assumption of Section 3. Furthermore, the notion of LGDBs from the main text is also included in *qoqo*, where they are called *decomposition blocks*. Hence, we have all the ingredients to build a tool to calculate the noisy algorithm model:

As an input, the code takes the noisy quantum circuit (i.e., including noise gates) implementing a Trotter step of the time evolution of a Spin system for which we want to find the noisy algorithm model would effectively be simulated on noisy hardware. Also as an input, the tool will receive the Trotter step size which is important for the correct rescaling of the Lindblad terms at the end.

In the noisy quantum circuit, every portion needs to be wrapped in decomposition blocks to signal that the respective gate sequences within the blocks correspond to the application of a exponential that is parametrically small (i.e., comparable or smaller than the Trotter step size). This is important information for the code to be able to commute noise through the circuit while staying within the error bars of the Trotter approximation. Furthermore, the decomposition blocks contain all the information about swapping operations, and whether the qubit indices the noise acts on need to be remapped when commuting noise past the block, to deal with the issue highlighted in 4.3.

We now go through the circuit starting with the first decomposition block. For this block, we get the list of the qubits that are involved in this block, as well as the list of operations, in order of execution. The code then goes through the list of operations, and finds the noise operations. For each noise operation, we build the Lindblad operator in a matrix form, and we convert the following gate operation to a physical operator. We can then commute the noise term past the gate operation, and we get a transformed noise

term, where the unitary transformation is defined by the unitary matrix that represents the gate, as shown in Eq. 37. We perform this every time we get to a gate operation, and need to commute the noise term past it, until we reach the end of the decomposition block.

Afterwards, the transformed noise terms will be commuted past the following decomposition blocks, where the qubit indices of the noise terms are remapped according to the remapping information of the blocks (stating if there are swapping operations contained in the block).

Finally, the noise terms are rescaled by the Trotter step size, as in the sum in Eq. 29 or Eq. 39.

This procedure is repeated for the second, third, etc., decomposition block in the noisy quantum circuit until we have treated every decomposition block in the circuit. Finally, the noise terms are added up following Eq. 29 and Eq. 39.

The output of our tool is then the sum of all the commuted though, and rescaled, noise terms. This corresponds to the Lindblad noise operator of the noisy algorithm model.

## D Error Analysis

When deriving the effective model being simulated by a given circuit, it is important to also consider the dominant sources of error in the approximations being made in the process. Before doing so, however, we must first clarify some notation. We assume that the Hamiltonian we wish to simulate possesses terms with some characteristic coupling scale  $J$ . The product of this coupling with the Trotter step size we will define as

$$\theta = J\tau. \quad (148)$$

For a super-operator corresponding to a coherent gate term, we define the scaled super-operator as

$$\mathcal{L}_G = J\bar{\mathcal{L}}_G \quad (149)$$

Thus, the quantity appearing in the exponential corresponding to a coherent gate is

$$\tau\mathcal{L}_G = \theta\bar{\mathcal{L}}_G \quad (150)$$

Likewise, we assume a characteristic noise scale  $\gamma$ , and define

$$\mu_G = \gamma t_G. \quad (151)$$

The scaled noise operator for a given gate is defined according to

$$\mathcal{L}_N^G = \gamma\bar{\mathcal{L}}_N^G \quad (152)$$

The argument appearing in the exponential is thus

$$t_G\mathcal{L}_N^G = \mu_G\bar{\mathcal{L}}_N^G \quad (153)$$

We also define a scaled version of the effective super-operator accordingly,

$$\tau\mathcal{L}_{\text{eff}} = \tau J\bar{\mathcal{L}}_{\text{eff}} = \theta\bar{\mathcal{L}}_{\text{eff}} \quad (154)$$

In our analysis, we will be interested in understanding corrections to  $\bar{\mathcal{L}}_{\text{eff}}$ , thus allowing us to more easily analyze the scaling of various errors.

We note that with these definitions, our zero order result can be written

$$\bar{\mathcal{L}}_{\text{eff}} \rightarrow \sum_X \bar{\mathcal{L}}_X + \sum_g (\mu_g/\theta) \bar{\mathcal{L}}_N^g. \quad (155)$$

### D.1 Higher Order Corrections in the BCH Formula

Thus far, when adding together all of the small parameter terms in a circuit, we have only carried out the BCH expansion to zero order. Now we would like to discuss the error which has been introduced by this approximation. When converting a product of exponentials into a single exponential,

$$\prod_i e^{A_i} = e^Z, \quad (156)$$

the BCH formula gives, to first order,

$$Z = \sum_i A_i + \frac{1}{2} \sum_{i<j} [A_i, A_j], \quad (157)$$

where  $i < j$  when  $A_i$  appears to the left of  $A_j$  in the product. The first term is of course the zero order contribution we have already considered, while the second term represents a first order correction. Since the circuits we consider will consist of small angle gates and noise terms, there are three types of commutators which will appear: gate terms with gate terms, gate terms with noise terms, and noise terms with noise terms. We consider each of these cases in turn.

First, it is clear that the commutator of two gate terms will produce another gate term. In particular,

$$[\bar{\mathcal{L}}_X, \bar{\mathcal{L}}_Y] = \bar{\mathcal{L}}_W, \quad (158)$$

where

$$\bar{\mathcal{L}}_Q \equiv -i [\bar{h}_Q, \cdot] \quad (159)$$

and

$$\bar{h}_W \equiv -i [\bar{h}_X, \bar{h}_Y]. \quad (160)$$

This is of course the usual correction to the coherent dynamics. Since each coherent term comes with a factor of  $\theta$  in the exponential, this leads to a correction to  $\bar{\mathcal{L}}_{\text{eff}}$  which scales as

$$\Delta(\theta\bar{\mathcal{L}}_{\text{eff}}) \sim \theta \cdot \theta \Rightarrow \Delta\bar{\mathcal{L}}_{\text{eff}} \sim \theta \quad (161)$$

Next, we consider commutators between gate terms and noise terms. In Appendix A we show that the commutator of a gate term with a noise term takes

the form of a noise term. Since each gate term carries a factor of  $\theta$ , and each noise term carries a factor of  $\mu_G$ , such a term leads to a correction of order

$$\Delta(\theta\bar{\mathcal{L}}_{\text{eff}}) \sim \theta \cdot \mu_G \Rightarrow \Delta\bar{\mathcal{L}}_{\text{eff}} \sim \mu_G \quad (162)$$

Since we assume  $\mu_G \ll \theta$ , in absolute terms, this represents a correction to the dynamics which is small compared with the previous correction we have found. If we instead focus only on the noisy part of the dynamics, such a term represents a correction to the noisy dynamics which is a factor  $\theta$  smaller than the order zero noisy dynamics. This relative scale is the same as for the correction to the coherent dynamics.

Lastly, we consider noise terms with noise terms. Such commutators have a mixed form - they do not necessarily take the form of a coherent correction or a noisy correction. Since each of these terms carries a factor of  $\mu_G$ , we find a correction which scales as

$$\Delta(\theta\bar{\mathcal{L}}_{\text{eff}}) \sim \mu_G \cdot \mu_G \Rightarrow \Delta\bar{\mathcal{L}}_{\text{eff}} \sim \mu_G^2/\theta \quad (163)$$

Again, since we assume  $\mu_G \ll \theta$ , we have in this case

$$\Delta\bar{\mathcal{L}}_{\text{eff}} \sim \mu_G^2/\theta \ll \theta^2/\theta = \theta \quad (164)$$

as well as

$$\Delta\bar{\mathcal{L}}_{\text{eff}} \sim \mu_G^2/\theta \ll (\mu_G\theta)/\theta = \mu_G, \quad (165)$$

and thus we find a correction which is significantly smaller than either of the two previous corrections.

Thus, we find the two most important corrections to the dynamics to be a coherent correction of order  $\theta$ , and a noisy correction of order  $\mu$ , each of which is a factor of  $\theta$  smaller than their respective zero order contributions.

## D.2 Corrections appearing in SWAP Blocks

When handling SWAP blocks, we have not thus far accounted for the effects of commuting a noise term past a small angle gate. Here, we wish to analyze the error introduced through this approximation.

We know that the modification of a noise term resulting from commuting it past a gate involves a correction to its underlying rate matrix which is given according to

$$\Gamma^N \rightarrow \Gamma^P \equiv M\Gamma^N M^\dagger \quad (166)$$

where

$$M = \eta^{-1}\chi; \quad \chi_{mn} \equiv \text{Tr}[A_m^\dagger U A_n U^\dagger]; \quad \eta_{mn} \equiv \text{Tr}[A_m^\dagger A_n] \quad (167)$$

When the gate in question is a small angle gate, we can approximate

$$U(J\tau) = \exp(-iJ\bar{h}\tau) \approx I - i\theta\bar{h} + \mathcal{O}(\theta^2) \quad (168)$$

Assuming for simplicity that we have chosen an orthonormal basis for  $\{A_n\}$ , our transformation becomes

$$\chi_{mn} \equiv \delta_{mn} + i\theta\Omega_{mn}, \quad (169)$$

where

$$\Omega_{mn} \equiv \text{Tr}[A_m^\dagger A_n \bar{h}] - \text{Tr}[A_m^\dagger \bar{h} A_n] \quad (170)$$

Thus, we find in this case

$$\begin{aligned} \Gamma^N \rightarrow \Gamma^P &\approx (I + i\theta\Omega)\Gamma^N(I - i\theta\Omega) \\ &\approx \Gamma^N + i\theta[\Omega, \Gamma^N] \end{aligned} \quad (171)$$

We have thus introduced an error of order  $\theta$  when neglecting the effects of commuting a noise term past a small angle gate, which is the same order as neglecting higher order terms in the BCH expansion. As a concrete example, if we consider a single qubit and take

$$\bar{h} = -\frac{1}{2}\sigma^x \quad (172)$$

then we have

$$\Omega = \lambda_7, \quad (173)$$

where  $\lambda_7$  is the seventh Gell-Mann matrix.

## D.3 Higher-Order Trotter Decompositions

In many situations, it is desirable to reduce the errors introduced through Trotterization by introducing a second order Trotter decomposition,

$$U(\tau) \approx \prod_{X=1}^Q U_X(\tau/2) \prod_{X=Q}^1 U_X(\tau/2) \quad (174)$$

where  $Q$  is the number of Hamiltonian terms. In other words, a trotter step of time  $\tau$  is implemented through a forwards sequence of gates, followed by the same sequence of gates in reverse. An example of such a circuit is shown in Figure 14. In such a case, each product  $U_X$  may need to be decomposed into a sequence of gates, each of which possessing its own noise term. Again, with a suitable set of manipulations, this circuit can be brought into the form of a sequence of SAGs, with noise terms interspersed among them. Our previously found formula for the effective model being simulated is still valid in this case. However, we must think more carefully about the dominant sources of error in this case.

By design, a second order Trotter decomposition is constructed such that any error in the coherent part of the Hamiltonian will scale as  $\mathcal{O}(\theta^2)$ . This is because the symmetric arrangement of terms implies that every commutator appearing in the expression for the first order correction is paired with another commutator in reverse order. Examining Figure 14, it is also clear that the same should hold true for the noise terms. If we assume that a given gate is always followed by the same noise term, and if we assume

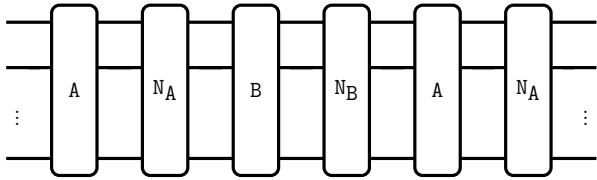


Figure 14: A very rough schematic of a second-order decomposition, with noise.

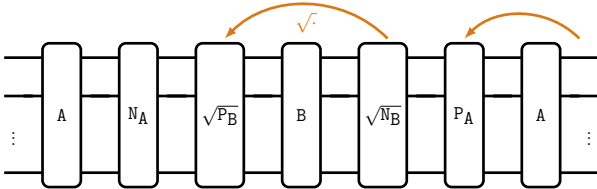


Figure 15: The idea of trying to symmetrize noise. The noise after gate B is split in half, with one half being commuted over. The noise after the second A gate is also commuted over. While this appears superficially symmetric, and as if the noise terms should now cancel, there are in fact order  $\theta$  corrections to the noise when commuting them, and so the cancellation is not perfect. This result in the same amount of error as if we had simply added them up in the original arrangement.

that a given term  $U_X$  is always decomposed using the same set of available gates, then after manipulating our circuit into one which possesses only SAGs and noise terms, the noise terms themselves should also be arranged symmetrically, and thus any first order contribution from commutators of noise terms with noise terms should also vanish (if these assumptions are not valid, then any asymmetry in the arrangement of noise terms will result in first order corrections which again scale as  $\mathcal{O}(\mu_G^2/\theta)$ .)

However, no such symmetry exists between gate terms and noise terms. In general, since we model noise terms as following gate terms, there will be imperfect cancellation among the commutators of gate terms with noise terms, leading again to a correction of order  $\mu_G$ . One might imagine that this could be remedied by modeling the noise differently in the second half of the circuit. If one models the noise terms as appearing before their corresponding gates in the second half of the circuit, the arrangement of gate terms and noise terms would again appear to be symmetric. However, when modeling noise as appearing before the corresponding gate, rather than after it, the nature of the noise term will then necessarily be different - in fact, we know that commuting a noise term past a SAG results in corrections of order  $\theta$  which, when combined with the overall effective noise scale  $\mu/\theta$ , will again lead to corrections of order  $\mu$ . Thus, even though noise and gate commutators appear in symmetric pairs, there is still an asymmetry of order  $\mu$ . This idea is demonstrated in Figure 15.

In such a second order circuit, we thus now have corrections to the noisy dynamics which scale as  $\mu$ , and corrections to the coherent dynamics which scale as  $\theta^2$ . We note that so long as  $\mu \ll \theta^2$ , the error in the noisy dynamics will still be small compared with the error introduced through Trotterization.

## References

- [1] Richard P. Feynman. Simulating physics with computers. *International Journal of Theoretical Physics*, 21(6):467–488, June 1982. ISSN 1572-9575. DOI: 10.1007/BF02650179. URL <https://doi.org/10.1007/BF02650179>.
- [2] Seth Lloyd. Universal Quantum Simulators. *Science*, 273(5278):1073–1078, August 1996. ISSN 0036-8075, 1095-9203. DOI: 10.1126/science.273.5278.1073. URL <https://www.science.org/doi/10.1126/science.273.5278.1073>.
- [3] I. M. Georgescu, S. Ashhab, and Franco Nori. Quantum simulation. *Reviews of Modern Physics*, 86(1):153–185, March 2014. DOI: 10.1103/RevModPhys.86.153. URL <https://link.aps.org/doi/10.1103/RevModPhys.86.153>. Publisher: American Physical Society.
- [4] Esteban A. Martinez, Christine A. Muschik, Philipp Schindler, Daniel Nigg, Alexander Erhard, Markus Heyl, Philipp Hauke, Marcello Dalmonte, Thomas Monz, Peter Zoller, and Rainer Blatt. Real-time dynamics of lattice gauge theories with a few-qubit quantum computer. *Nature*, 534(7608):516–519, June 2016. ISSN 1476-4687. DOI: 10.1038/nature18318. URL <https://www.nature.com/articles/nature18318>. Number: 7608 Publisher: Nature Publishing Group.
- [5] Abhinav Kandala, Antonio Mezzacapo, Kristan Temme, Maika Takita, Markus Brink, Jerry M. Chow, and Jay M. Gambetta. Hardware-efficient variational quantum eigensolver for small molecules and quantum magnets. *Nature*, 549(7671):242–246, September 2017. ISSN 1476-4687. DOI: 10.1038/nature23879. URL <https://www.nature.com/articles/nature23879>. Number: 7671 Publisher: Nature Publishing Group.
- [6] Abhinav Kandala, Kristan Temme, Antonio D. Córcoles, Antonio Mezzacapo, Jerry M. Chow, and Jay M. Gambetta. Error mitigation extends the computational reach of a noisy quantum processor. *Nature*, 567(7749):491–495, March 2019. ISSN 1476-4687. DOI: 10.1038/s41586-019-1040-7. URL <https://www.nature.com/articles/s41586-019-1040-7>. Number: 7749 Publisher: Nature Publishing Group.
- [7] Frank Arute, Kunal Arya, Ryan Babbush, Dave Bacon, Joseph C. Bardin, Rami Barends,

- Andreas Bengtsson, Sergio Boixo, Michael Broughton, Bob B. Buckley, David A. Buell, Brian Burkett, Nicholas Bushnell, Yu Chen, Zijun Chen, Yu-An Chen, Ben Chiaro, Roberto Collins, Stephen J. Cotton, William Courtney, Sean Demura, Alan Derk, Andrew Dunsworth, Daniel Eppens, Thomas Eckl, Catherine Erickson, Edward Farhi, Austin Fowler, Brooks Foxen, Craig Gidney, Marissa Giustina, Rob Graff, Jonathan A. Gross, Steve Habegger, Matthew P. Harrigan, Alan Ho, Sabrina Hong, Trent Huang, William Huggins, Lev B. Ioffe, Sergei V. Isakov, Evan Jeffrey, Zhang Jiang, Cody Jones, Dvir Kafri, Kostyantyn Kechedzhi, Julian Kelly, Seon Kim, Paul V. Klimov, Alexander N. Korotkov, Fedor Kostritsa, David Landhuis, Pavel Laptev, Mike Lindmark, Erik Lucero, Michael Marthaler, Orion Martin, John M. Martinis, Anika Marusczyk, Sam McArdle, Jarrod R. McClean, Trevor McCourt, Matt McEwen, Anthony Megrant, Carlos Mejuto-Zaera, Xiao Mi, Masoud Mohseni, Wojciech Mruczkiewicz, Josh Mutus, Ofer Naaman, Matthew Neeley, Charles Neill, Hartmut Neven, Michael Newman, Murphy Yuezhen Niu, Thomas E. O'Brien, Eric Ostby, Bálint Pató, Andre Petukhov, Harald Putterman, Chris Quintana, Jan-Michael Reiner, Pedram Roushan, Nicholas C. Rubin, Daniel Sank, Kevin J. Satzinger, Vadim Smelyanskiy, Doug Strain, Kevin J. Sung, Peter Schmitteckert, Marco Szalay, Norm M. Tubman, Amit Vainsencher, Theodore White, Nicolas Vogt, Z. Jamie Yao, Ping Yeh, Adam Zalcman, and Sebastian Zanker. Observation of separated dynamics of charge and spin in the Fermi-Hubbard model, October 2020. URL <http://arxiv.org/abs/2010.07965>. arXiv:2010.07965 [quant-ph].
- [8] Austin G. Fowler, Matteo Mariantoni, John M. Martinis, and Andrew N. Cleland. Surface codes: Towards practical large-scale quantum computation. *Physical Review A*, 86(3):032324, September 2012. DOI: [10.1103/PhysRevA.86.032324](https://doi.org/10.1103/PhysRevA.86.032324). URL <https://link.aps.org/doi/10.1103/PhysRevA.86.032324>. Publisher: American Physical Society.
- [9] Simon J. Devitt, William J. Munro, and Kae Nemoto. Quantum error correction for beginners. *Reports on Progress in Physics*, 76(7):076001, June 2013. ISSN 0034-4885. DOI: [10.1088/0034-4885/76/7/076001](https://doi.org/10.1088/0034-4885/76/7/076001). URL <https://doi.org/10.1088/0034-4885/76/7/076001>. Publisher: IOP Publishing.
- [10] Bjoern Lekitsch, Sebastian Weidt, Austin G. Fowler, Klaus Mølmer, Simon J. Devitt, Christof Wunderlich, and Winfried K. Hensinger. Blueprint for a microwave trapped ion quantum computer. *Science Advances*, 3(2):e1601540, February 2017. DOI: [10.1126/sciadv.1601540](https://doi.org/10.1126/sciadv.1601540). URL <https://www.science.org/doi/10.1126/sciadv.1601540>. Publisher: American Association for the Advancement of Science.
- [11] Kishor Bharti, Alba Cervera-Lierta, Thi Ha Kyaw, Tobias Haug, Sumner Alperin-Lea, Abhinav Anand, Matthias Degroote, Hermann Heimonen, Jakob S. Kottmann, Tim Menke, Wai-Keong Mok, Sukin Sim, Leong-Chuan Kwek, and Alán Aspuru-Guzik. Noisy intermediate-scale quantum algorithms. *Reviews of Modern Physics*, 94(1):015004, February 2022. DOI: [10.1103/RevModPhys.94.015004](https://doi.org/10.1103/RevModPhys.94.015004). URL <https://link.aps.org/doi/10.1103/RevModPhys.94.015004>. Publisher: American Physical Society.
- [12] Zhenyu Cai, Ryan Babbush, Simon C. Benjamin, Suguru Endo, William J. Huggins, Ying Li, Jarrod R. McClean, and Thomas E. O'Brien. Quantum Error Mitigation, October 2022. URL <http://arxiv.org/abs/2210.00921>. arXiv:2210.00921 [quant-ph].
- [13] Vincent Russo, Andrea Mari, Nathan Shammah, Ryan LaRose, and William J. Zeng. Testing platform-independent quantum error mitigation on noisy quantum computers, October 2022. URL <http://arxiv.org/abs/2210.07194>. arXiv:2210.07194 [quant-ph].
- [14] Jan-Michael Reiner, Sebastian Zanker, Iris Schwenk, Juha Leppäkangas, Frank Wilhelm-Mauch, Gerd Schön, and Michael Marthaler. Effects of gate errors in digital quantum simulations of fermionic systems. *Quantum Science and Technology*, 3(4):045008, August 2018. ISSN 2058-9565. DOI: [10.1088/2058-9565/aad5ba](https://doi.org/10.1088/2058-9565/aad5ba). URL <https://iopscience.iop.org/article/10.1088/2058-9565/aad5ba>.
- [15] Kushal Seetharam, Debopriyo Biswas, Crystal Noel, Andrew Risinger, Daiwei Zhu, Or Katz, Sambuddha Chattopadhyay, Marko Cetina, Christopher Monroe, Eugene Demler, and Dries Sels. Digital quantum simulation of NMR experiments, September 2021. URL <http://arxiv.org/abs/2109.13298>. arXiv:2109.13298 [physics, physics:quant-ph].
- [16] S. I. Doronin, E. B. Fel'dman, E. I. Kuznetsova, and A. I. Zenchuk. Simulation of multiple-quantum NMR dynamics of spin dimer on quantum computer, April 2021. URL <http://arxiv.org/abs/2104.13777>. arXiv:2104.13777 [quant-ph].
- [17] Michael A. Nielsen and Isaac L. Chuang. Quantum Computation and Quantum Information: 10th Anniversary Edition, December 2010. URL <https://www.cambridge.org/highereducation/books/quantum-computation-and-quantum-information/01E10196D0A682A6AEFFEA52D53BE9AE>. ISBN:

- 9780511976667 Publisher: Cambridge University Press.
- [18] H. F. Trotter. On the product of semi-groups of operators. Proceedings of the American Mathematical Society, 10(4):545–551, 1959. ISSN 0002-9939, 1088-6826. DOI: 10.1090/S0002-9939-1959-0108732-6. URL <https://www.ams.org/proc/1959-010-04/S0002-9939-1959-0108732-6/>.
- [19] Masuo Suzuki. Generalized Trotter’s formula and systematic approximants of exponential operators and inner derivations with applications to many-body problems. Communications in Mathematical Physics, 51(2):183–190, June 1976. ISSN 1432-0916. DOI: 10.1007/BF01609348. URL <https://doi.org/10.1007/BF01609348>.
- [20] Naomichi Hatano and Masuo Suzuki. Finding Exponential Product Formulas of Higher Orders. In Arnab Das and Bikas K. Chakrabarti, editors, Quantum Annealing and Other Optimization Methods, Lecture Notes in Physics, pages 37–68. Springer, Berlin, Heidelberg, 2005. ISBN 978-3-540-31515-5. DOI: 10.1007/11526216\_2. URL [https://doi.org/10.1007/11526216\\_2](https://doi.org/10.1007/11526216_2).
- [21] Göran Lindblad. On the Generators of Quantum dynamical semigroups. Commun. Math. Phys., 48:119, 1976.
- [22] Daniel A. Lidar. Lecture notes on the theory of open quantum systems, 2019. URL <https://arxiv.org/abs/1902.00967>.
- [23] H.P. Breuer, F. Petruccione, and S.P.A.P.F. Petruccione. The Theory of Open Quantum Systems. Oxford University Press, 2002. ISBN 9780198520634.
- [24] Julio T. Barreiro, Markus Müller, Philipp Schindler, Daniel Nigg, Thomas Monz, Michael Chwalla, Markus Hennrich, Christian F. Roos, Peter Zoller, and Rainer Blatt. An open-system quantum simulator with trapped ions. Nature, 470(7335):486–491, February 2011. ISSN 1476-4687. DOI: 10.1038/nature09801. URL <https://www.nature.com/articles/nature09801>. Number: 7335 Publisher: Nature Publishing Group.
- [25] Zixuan Hu, Rongxin Xia, and Sabre Kais. A quantum algorithm for evolving open quantum dynamics on quantum computing devices. Scientific Reports, 10(1):3301, February 2020. ISSN 2045-2322. DOI: 10.1038/s41598-020-60321-x. URL <https://www.nature.com/articles/s41598-020-60321-x>. Number: 1 Publisher: Nature Publishing Group.
- [26] Anthony W. Schlingens, Kade Head-Marsden, LeeAnn M. Sager, Prineha Narang, and David A. Mazziotti. Quantum Simulation of Open Quantum Systems Using a Unitary Decomposition of Operators. Physical Review Letters, 127(27):270503, December 2021. ISSN 0031-9007, 1079-7114. DOI: 10.1103/PhysRevLett.127.270503. URL <http://arxiv.org/abs/2106.12588>. arXiv:2106.12588 [physics, physics:quant-ph].
- [27] Minjae Jo and Myungshik Kim. Simulating open quantum many-body systems using optimised circuits in digital quantum simulation, March 2022. URL <http://arxiv.org/abs/2203.14295>. arXiv:2203.14295 [cond-mat, physics:quant-ph].
- [28] O. Astafiev, Yu. A. Pashkin, Y. Nakamura, T. Yamamoto, and J. S. Tsai. Quantum Noise in the Josephson Charge Qubit. Physical Review Letters, 93(26):267007, December 2004. DOI: 10.1103/PhysRevLett.93.267007. URL <https://link.aps.org/doi/10.1103/PhysRevLett.93.267007>. Publisher: American Physical Society.
- [29] Radoslaw C. Bialczak, R. McDermott, M. Ansmann, M. Hofheinz, N. Katz, Erik Lucero, Matthew Neeley, A. D. O’Connell, H. Wang, A. N. Cleland, and John M. Martinis.  $1/f$  Flux Noise in Josephson Phase Qubits. Physical Review Letters, 99(18):187006, November 2007. DOI: 10.1103/PhysRevLett.99.187006. URL <https://link.aps.org/doi/10.1103/PhysRevLett.99.187006>. Publisher: American Physical Society.
- [30] L. Cardani, F. Valenti, N. Casali, G. Cate-lani, T. Charpentier, M. Clemenza, I. Colan-toni, A. Cruciani, G. D’Imperio, L. Gironi, L. Grünhaupt, D. Gusenkova, F. Henriques, M. Lagoïn, M. Martinez, G. Pettinari, C. Rusconi, O. Sander, C. Tomei, A. V. Ustinov, M. Weber, W. Wernsdorfer, M. Vignati, S. Pirro, and I. M. Pop. Reducing the impact of radioactivity on quantum circuits in a deep-underground facility. Nature Communications, 12(1):2733, May 2021. ISSN 2041-1723. DOI: 10.1038/s41467-021-23032-z. URL <https://www.nature.com/articles/s41467-021-23032-z>. Number: 1 Publisher: Nature Publishing Group.
- [31] Sergio Boixo, Sergei V. Isakov, Vadim N. Smelyanskiy, Ryan Babbush, Nan Ding, Zhang Jiang, Michael J. Bremner, John M. Martinis, and Hartmut Neven. Characterizing quantum supremacy in near-term devices. Nature Physics, 14(6):595–600, June 2018. ISSN 1745-2481. DOI: 10.1038/s41567-018-0124-x. URL <https://www.nature.com/articles/s41567-018-0124-x>. Number: 6 Publisher: Nature Publishing Group.
- [32] Tetsuji Kimura. Explicit description of the Zassenhaus formula. Progress of Theoretical and Experimental Physics, 2017(4), 04 2017. ISSN 2050-3911. DOI: 10.1093/ptep/ptx044.

URL <https://doi.org/10.1093/ptep/ptx044.041A03>.

[33] GitHub - HQSquantumsimulations/qoqo, .  
URL <https://github.com/HQSquantumsimulations/qoqo>.

[34] QuEST – Quantum Exact Simulation Toolkit, .  
URL <https://quest.qtechtheory.org/>.